Interreg

Sofinancira EVROPSKA UNIJA
Kofinanziert von der EUROPÄISCHEN UNION

Slovenija – Österreich

ADDCIRCLES

AM CONNECT: International Conference on Research and Industrial Advances in Additive Manufacturing

3 and 4 December 2025
Carinthia University of Applied Sciences, Villach / Beljak, Austria

PROCEEDINGS

More information about the conference on

Imprint

Publisher
ADMiRE Research Center, Carinthia University of Applied Sciences, Austria
in cooperation with the Faculty of Polymer Technology, Slovenia

Title
Proceedings of the 1st International Conference on Research and Industrial Advances in Additive Manufacturing 2025 (AM Connect 2025)

Editors
Sandra Schulnig, Mathias Brandstötter, Janez Slapnik, Maja Mešl

Year of publication
2025

Publication type
annual**,** no print edition

ISBN
978-3-99076-113-7

PROJECT: SIAT00036 – ADDCIRCLES
ADDCIRCLES - Promoting Sustainable Regional Development through Additive Manufacturing:
A Cross-Border Initiative for a Resilient and Circular Economy

URL: https://www.ammap.eu

About AM Connect

AM Connect is a two-day cross-border event on Additive Manufacturing (AM) that brings together industry representatives and researchers from Austria and Slovenia. The conference focuses on industrial applications, current research, and cross-border collaboration, and is organised within the ADDCIRCLES project under the INTERREG SI–AT programme, co-funded by the European Regional Development Fund.

The conference aims to:

- Share knowledge and expertise in AM across borders
- Create networking opportunities between industry and research institutions
- Strengthen the Slovenia–Austria AM community
- Explore current developments and future trends in AM
- Highlight innovative AM projects and solutions
- Provide exhibition opportunities for industry stakeholders

Target group: Industry professionals and researchers working in Additive Manufacturing

Conference Topics

The technical program is structured around the following themes:

- Smart Additive Manufacturing – AI, Process Monitoring & Digital Twins
- AM for High-Impact Applications
- Industrial-Scale Additive Manufacturing – From Prototyping to Production
- Process Innovations in Additive Manufacturing
- Advanced Materials for Next-Generation Additive Manufacturing
- Performance & Performance Enhancement in Additive Manufacturing
- European and National AM Projects and Initiatives

Scientific Committee

- Sandra Schulnig, CUAS
- Mathias Brandstötter, CUAS
- Janez Slapnik, FTPO
- Dragan Kusić, TECOS
- Surisetty Jyothsna, Wood K plus
- Johannes Gartner, TU Delft
- Clemens Holzer, Montanuniversitaet Leoben
- Joamin Gonzalez-Gutierrez, Luxembourg Institute of Science and Technology
- Igor Drstvenšek, University of Maribor

Organizing Committee

- Sandra Schulnig, CUAS
- Mathias Brandstötter, CUAS
- Zala Lorber, FTPO
- Maja Mešl, FTPO
- Simona Knežević Vernon, TECOS
- Ram Dušić Hren, TECOS
- Surisetty Jyothsna, Wood K plus
- Agnes Parfy, AM Austria
- Johannes Gartner, AM Austria
- Branka Mušič, ZAG
- Thomas Petschnig, GPS

Program Overview

Day 1 – 3 December 2025

Industry & Innovation Focus – Advancing Industrial Applications & Business Opportunities in AM

08:15–09:00 – Registration & Coffee
09:00–09:30 – Opening Session with Representatives from Regional Authorities
09:30–10:15 – Keynote 1 – Politics Meets Production: The Future of Additive Manufacturing in the EU | Johannes Gartner
10:15–10:45 – Exhibitor Spotlight
11:15–13:00 – Session 1: Smart Additive Manufacturing – AI, Process Monitoring & Digital Twins
14:00–15:15 – Session 2: AM for High-Impact Applications
15:45–17:00 – Session 3: Industrial-Scale Additive Manufacturing – From Prototyping to Production
17:00–18:30 – Exhibition & AM World Café
19:30–22:00 – Conference Dinner

Day 2 – 4 December 2025

Research, Projects & Initiatives – Cutting-Edge Research & Emerging Innovations

08:30–09:00 – Registration & Coffee
09:00–09:45 – Keynote 2 – Advancing Human Health Through Design for Additive Manufacturing | Serena Graziosi
09:45–11:15 – Session 5: Process Innovations in Additive Manufacturing
11:45–13:15 – Session 6: Advanced Materials for Next-Generation AM
14:35–16:05 – Session 7: Performance & Performance Enhancement in AM
16:05–17:15 – Session 8: European & National AM Projects & Initiatives
17:15–17:30 – Closing Session & Farewell Networking

Day 1 – Industry & Innovation Focus

Keynote 1: Politics Meets Production: The Future of Additive Manufacturing in the EU

Johannes Gartner, Delft University of Technology, NL

Johannes Gartner discusses how European industrial policy, innovation funding and regulation interact with the rapid development of Additive Manufacturing. The keynote explores AM as a strategic technology for resilience, competitiveness and sustainability in European industry, linking political initiatives and industrial needs. Particular emphasis is placed on how cross-border platforms, standards and ecosystems can help Europe move from pilot projects to large-scale industrial impact.

SESSION 1 – SMART ADDITIVE MANUFACTURING – AI, PROCESS MONITORING & DIGITAL TWINS

What Can Boost Competitiveness of Additive Manufacturing? – New Processes, New Machines, New Materials

Franz Haas, Institute of Production Engineering, Graz University of Technology, AT

This talk outlines three major levers for making AM more competitive: process innovations, machine concepts and advanced materials. Examples include novel powder-based processes, hybrid machine architectures and research on materials such as magnesium alloys for laser powder bed fusion. The contribution highlights how coordinated advances in all three dimensions are essential to reduce cost, improve quality and open new application fields.

Inline Process Monitoring Systems for Additive Manufacturing of Metals – Added Value for Detection of Flaws and Predictive Maintenance

Thomas Grünberger, LKR Ranshofen, AT

Grünberger presents inline monitoring concepts for metal AM, combining sensor systems with data analysis to detect defects during production. The contribution discusses how process signatures can be used for early identification of flaws, assessment of component quality and predictive maintenance of AM equipment. Use cases illustrate benefits for reduced scrap rates and more stable industrial production.

Monitoring and Closed-Loop Control of the DMLS Process to Improve the Microstructure and Mechanical Properties
Aydın Yağmur, EOS GmbH, DE

This presentation focuses on selective laser melting / direct metal laser sintering (DMLS) and shows how real-time monitoring and feedback control can be employed to steer energy input and solidification behaviour. By linking process parameters to microstructure and mechanical performance, the work aims to enable adaptive control strategies that ensure consistent part properties across builds and machines.

Prediction of the Fatigue Lifetime of Components Produced via Endless Fibre Reinforced Extrusion-Based Additive Manufacturing
Florian Arbeiter, Montanuniversitaet Leoben, AT

Florian Arbeiter discusses extrusion-based AM of continuous fibre-reinforced components and the challenges of predicting their fatigue behaviour. The contribution considers material models, load scenarios and experimental testing, with the goal of establishing design-relevant lifetime predictions. This supports the use of endless-fibre AM parts in safety-critical or long-life applications.

SESSION 2 – AM FOR HIGH-IMPACT APPLICATIONS

About Additive Manufacturing Designs in the Hot Core of an Aircraft Engine
Fabrice Giuliani, Combustion Bay One e.U., AT

Giuliani reviews design concepts for AM components operating in the hot section of gas turbines and aircraft engines, such as combustor parts or nozzles. The talk highlights how AM-enabled geometries can improve thermal management, flow control and weight, while also addressing constraints such as material performance, certification and manufacturability.

Innovation vs. Tradition: The Role of Additively Manufactured Metal Implants in Modern Medicine
Igor Drstvenšek, University of Maribor, SI

This contribution contrasts conventional manufacturing routes for medical implants with AM-based solutions. It emphasises personalised geometries, lattice structures and surface adaptations enabled by AM, and discusses clinical opportunities and regulatory hurdles. The talk illustrates how AM complements, rather than simply replaces, traditional implant production.

Additive Manufacturing of High-Performance Ceramic Materials
Martin Schwentenwein, Lithoz GmbH, AT

Schwentenwein presents ceramic AM technologies capable of producing dense, high-performance oxide and non-oxide ceramics. The contribution covers material development, process chains, sintering and achievable properties, with application examples from healthcare, energy and industry where ceramics' thermal and chemical robustness are essential.

SESSION 3 – INDUSTRIAL-SCALE AM – FROM PROTOTYPING TO PRODUCTION

Scalability of Production Using Hybrid Additive Manufacturing and Injection Moulding for Low-Batch Applications
Alen Šapek, Additio d.o.o., SI

This talk explores process chains that combine polymer AM with injection moulding to economically serve low-volume production. By using AM to create inserts, tools or preforms, and injection moulding for the final parts, companies can scale from prototypes to small series without investing in full conventional tooling. Practical examples illustrate cost and lead-time benefits.

Parametric Design Meets Robotics in Custom Additive Manufacturing
Johannes Braumann, University of Arts Linz, AT

Braumann discusses workflows where parametric design tools are coupled with robotic fabrication for highly customised AM parts. The presentation highlights toolpath-aware geometry generation, robot kinematics and material behaviour, showing how digital design and robotic deposition can be integrated for bespoke components in architecture, design and industry.

From Vision to Value: Large-Format Additive Manufacturing
Erik Paessler, CEAD B.V., NL

Paessler addresses large-format thermoplastic extrusion systems and their role in producing sizeable tools, moulds and structural parts. Topics include machine architecture, process window, materials and quality assurance. Case studies demonstrate how large-format AM can shorten development cycles and replace or complement traditional fabrication of big structures.

Day 2 – Research, Projects & Initiatives

Keynote 2: Advancing Human Health Through Design for Additive Manufacturing

Prof. Serena Graziosi, Politecnico di Milano, IT

Serena Graziosi highlights the role of design for AM in creating medical devices and health-related products that are lighter, more functional and better tailored to patients. The keynote covers topology optimisation, lattice structures, and patient-specific geometries, alongside regulatory and validation aspects that must be addressed to bring AM-designed medical products safely into clinical use.

SESSION 5 – PROCESS INNOVATIONS IN ADDITIVE MANUFACTURING

Dynamic Photopolymers: Paving the Way for Sustainable 3D Printing

Elisabeth Rossegger, Polymer Competence Center Leoben & Graz University of Technology, AT

Rossegger presents dynamic photopolymer networks for vat photopolymerisation, aimed at improving recyclability, repairability and lifetime of printed parts. By introducing reversible bonds and adaptable polymer architectures, these materials enable reprocessing and healing while maintaining performance, supporting more circular use of photopolymers in AM.

Multi-Criteria Approach for Multi-Axis Printing in Additive Manufacturing

Julian Bosch, EOS GmbH, DE, with co-authors from CUAS and KED-Engineering, AT

Bosch proposes a decision framework for choosing between conventional 3-axis fused-filament fabrication and multi-axis printing strategies. Criteria such as surface quality, support requirements, build time and reachable geometries are considered. The contribution explains how a decision criterion can guide users towards the most suitable printing approach for complex parts.

Additive manufacturing of high-performance materials. Advanced alloys and beyond

Ivan Goncharov, Alfonso Additive, IT

Goncharov discusses additive manufacturing strategies for high-performance materials, drawing on projects in powder metallurgy and AM. He compares advanced powder production routes with AM processes for steels, superalloys, intermetallics, high-entropy alloys and ceramics, aiming to show how tailored powders and AM enable components for extreme environments beyond the reach of conventional processing.

Towards Full-Field Thermal Monitoring During Additive Manufacturing Process Using Simulation- & ML-Based Virtual Sensing

Monika Stipsitz, Silicon Austria Labs GmbH, AT

This contribution investigates combining physics-based thermal simulations with machine-learning-based virtual sensing to reconstruct temperature fields inside a part during AM. By fusing limited sensor data with models, the method aims to deliver full-field thermal information in near real time, which could be used for process control and quality assurance.

SESSION 6 – ADVANCED MATERIALS FOR NEXT-GENERATION AM

New Advances on Additive Manufacturing of Al Alloys for Space Applications

Riccardo Casati, Politecnico di Milano, IT

Casati presents recent research on aluminium alloys tailored for space applications and processed by AM. The talk discusses alloy design, process parameter optimisation and post-treatments to achieve high strength, reliability and performance under demanding service conditions such as vacuum, radiation and thermal cycling.

functionalWOOD2print – Binder-Jet 3D Printing of Tough Biobased Structural Materials with Functional Surfaces

Doris Kapl, Wood K plus, AT, with co-authors

This work explores binder-jetting of wood-based powders and bio-based mixtures to create structural components with functionalised surfaces. The contribution details powder selection, flowability, infiltration strategies and mechanical performance, as well as the potential for integrating additional functionalities while maintaining a largely bio-based material system.

Sustainability in Additive Manufacturing – Influence of Powder Reuse on High-Temperature Strength in L-PBF of Ti-6Al-4V

Benjamin Meier-Leeb, Carinthia University of Applied Sciences, AT

This contribution studies how repeated reuse of Ti-6Al-4V powder in laser powder bed fusion affects the high-temperature mechanical behaviour of printed parts. By examining microstructure and strength after different reuse cycles, the work aims to balance sustainability—through powder reuse—with the need for reliable, high-performance components.

Mechanical Properties of Carbon and Natural Fibers – TPU Composites for Additive Manufacturing Applications

Jaka Vaupot, ZAG & Jožef Stefan International Postgraduate School, SI, with co-authors

Vaupot investigates thermoplastic polyurethane composites reinforced with carbon and natural fibres for extrusion-based AM. The study addresses compounding, printability and resulting mechanical performance, comparing synthetic and natural reinforcement. The goal is to move towards more sustainable yet mechanically capable filament materials for structural AM applications.

Unlocking New Functionalities and Improved Properties in Material Extrusion Additive Manufacturing Through Dynamic Covalent Chemistry

Janez Slapnik, Faculty of Polymer Technology, SI

This talk focuses on polymers for material-extrusion AM that incorporate dynamic covalent bonds. Such materials can enable self-healing, reprocessing and adaptive mechanical behaviour. The contribution discusses material design, processing windows and how dynamic chemistry can be harnessed without compromising printability or dimensional stability.

SESSION 7 – PERFORMANCE & PERFORMANCE ENHANCEMENT IN AM

Design Optimisation for Additive Manufacturing

Damir Godec, University of Zagreb, HR

Godec reviews design-for-AM and optimisation strategies that leverage the geometric freedom of AM while respecting manufacturing constraints. Examples include topology optimisation, lattice design and part consolidation, illustrated with industrial case studies. The talk emphasises the importance of integrating design optimisation with process knowledge to fully exploit AM's potential.

Tuning Quasi-Zero Stiffness in Additively Manufactured Kresling Structures via Silicone Encapsulation and Infill Design

Carina Emminger, Johannes Kepler University Linz, AT, with co-authors

This contribution examines origami-inspired Kresling structures produced by material-extrusion AM and subsequently encapsulated in silicone elastomers. By varying infill parameters and silicone layer properties, the authors tune quasi-zero-stiffness regions in the force–displacement response. Potential applications include vibration isolation and adaptive mechanical systems.

Tailor-Made Conductive Thermoplastic Filaments for Extrusion-Based FDM Printed Strain Sensing in Thermoset Composites

Arunjunai Raj Mahendran, Wood K plus, AT

Mahendran's talk addresses the development of electrically conductive thermoplastic filaments that can be printed onto or into thermoset composite structures to act as strain-sensing elements. The contribution covers materials formulation, processing and basic electromechanical characterisation, illustrating how AM can be used to integrate sensing directly into structural components.

The Effect of the Number of Thermal Cycles on the Mechanical Properties of Parts Fabricated by Laser Powder Bed Fusion

Snehashis Pal, University of Maribor, SI

Pal investigates how repeated thermal cycling during laser powder bed fusion—caused, for instance, by complex scan strategies or multi-layer reheating—affects the mechanical properties of printed parts. The study discusses changes in microstructure, residual stresses and strength, and points to strategies for controlling or mitigating detrimental thermal-cycle effects.

SESSION 8 – EUROPEAN & NATIONAL AM PROJECTS & INITIATIVES

This closing session presents selected European and national projects related to Additive Manufacturing, including Horizon Europe and INTERREG initiatives. It highlights cross-border collaborations between Slovenia and Austria, outlines project goals and main achievements, and invites participants to engage in future joint activities and funding opportunities.

Scientific Papers and Extended Abstracts

Multi-Criteria Approach for Multi-Axis Printing in Additive Manufacturing

Julian Bosch*[1], Mathias Brandstötter[2], Ziad Khalil[3]

EOS GmbH, Robert-Stirling-Ring 1, 82152 Krailling, Germany[1]
ADMiRE Research Center, Carinthia University of Applied Sciences,
Europastraße 4, 9524 Villach, Austria[2]
KED-Engineering Ingenieurbüro Maschinenbau, Industriezeile 54,
5280 Braunau am Inn, Austria[3]
Corresponding Author: julian.bosch@eos.info*

***Abstract*—This work presents a systematic approach to defining a decision criterion (DC) for choosing between conventional 3-axis Fused Deposition Modeling (3A-FFF) and advanced Multi-Axis FFF (MA-FFF). While 3A-FFF is limited in handling complex geometries, MA-FFF offers greater design flexibility and improved mechanical properties through additional degrees of freedom. However, a structured framework to determine when MA-FFF is advantageous has been missing. The proposed methodology evaluates kinematics, printing strategies, and economic factors across three modules: identifying feasible processes, defining evaluation criteria, and applying a weighted decision matrix. Its effectiveness is demonstrated with a curved pipe case study, comparing FFF strategies in terms of cost, quality, productivity, and mechanical performance. Results show MA-FFF's potential for specific applications, though progress in slicing software remains essential to fully exploit its benefits. The paper concludes with practical implications and future directions to support industrial adoption of MA-FFF.**

I. Introduction

Additive manufacturing (AM), particularly the 3 Axis Fused Deposition Modeling (3A-FFF) process, has established itself as a fundamental and successful manufacturing technique across various industries in recent years [1, 2]. Its flexibility, cost-effectiveness, and ability to produce diverse geometries make the 3A-FFF process suitable for prototype development, and small-scale manufacturing. Despite these successes, the 3A-FFF process faces limitations, particularly in producing parts with complex geometries or high load-bearing requirements.

A promising extension of the 3A-FFF process is the Multi Axis Fused Deposition Modeling (MA-FFF) technology [3], which offers greater design freedom and improved mechanical properties. Although research and initial commercialization exist, clear criteria for its efficient application are still lacking. Current studies show that MA-FFF can outperform 3A-FFF in mechanical properties, post-processing, or material use [4–6]. However, there is a lack of comprehensive understanding regarding the conditions under which MA-FFF technology is superior and when traditional 3A-FFF might yield comparable or even better results.

The aim of this work is to bridge this gap and provide a clear distinction between the two methods. By analyzing kinematics, printing techniques, and economic aspects, a reproducible methodology will be developed to evaluate which process is most suitable for the production of specific components. The significance of this research lies in establishing a scientifically grounded decision criterion (DC) for FFF printing strategies.

II. Limitations of 3A-FFF

The stair-stepping effect, resulting from the layer-by-layer deposition of material, is one of the most well-known defects in 3A-FFF printing, produces visible steps that reduce surface quality [7, 8]. Many printing errors in the 3A-FFF process arise from the influence of gravity, as the extruded material, due to its low viscosity, does not form self-supporting structures [9]. This particularly leads to deformations and inaccuracies in print details for overhangs, cantilevers, and bridges. While smaller bridges (15-25 mm) and overhangs up to 40° can be printed without significant errors, larger geometries necessitate the use of additional support structures [10–13]. The support structures are a crucial but limiting component of the 3A-FFF process. They enable the printing of complex geometries like overhangs but increase material consumption, printing time, and require post-processing for removal, which incurs additional costs [14, 15, 16].

II. Decision criteria

The decision criteria (DC) was derived using a structured utility value analysis approach. Based on literature review and expert evaluation, qualitative and quantitative criteria such as cost, part quality, productivity, and mechanical performance were selected.

Each criterion was weighted according to its relevance for industrial FDM applications. The resulting weighted decision matrix enables consistent process selection by linking measurable performance data with qualitative assessments.

The DC is located in the pre-process of the production sequence. The pre-process characterizes the initial phase, which includes all preparatory measures, from evaluating the print file to setting up the machine before the actual printing process. In particular, the DC is positioned here between the evaluation of the 3D data and the generation of the machine code. At this point, the decision must be made as to which specific printing process will be selected for the component. The pre-process thus forms the framework in which the DC is applied.

The approach to developing the DC represents a systematic approach to solving a multi-criteria decision problem. Clearly defined steps are followed, which act as a deterministic algorithm and lead to consistent results with the same input parameters [17]. The DC is divided into three main module parts, which make it possible to identify the optimal production process based on various criteria.

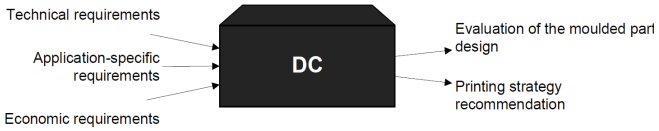

Fig. 1. The DC as a black box.

III. 5.3 Practical Application and Demonstration

The demonstrator component is a curved pipe that serves as a thin-walled connector for a ventilation duct. The 3D view of the part is shown in Fig. 2. Costs are weighted at 50% due to their critical impact on economic viability. Part quality is weighted at 25% to ensure the necessary surface finish. Productivity is weighted at 15% to adhere to the tight schedule. Mechanical requirements are weighted at 10% to ensure the structural integrity of the component.

Tab. 1. Decision matrix for the curved ventilation pipe.

Decision matrix curved ventilation pipe						
	Weighting	3A-FDM	ILP	Curved structures	Axial MA-FDM	Non-planar surfaces
Costs	50%	4,7	4,8	5	3,2	-
		2,4	2,4	2,5	1,6	-
Part quality	25%	2,0	3,0	5,0	5,0	-
		0,5	0,8	1,3	1,3	-
Productivity	15%	4,0	3,0	4,0	1,0	-
		0,6	0,5	0,6	0,2	-
Mech. Properties	10%	1,0	1,0	2,0	5,0	-
		0,1	0,1	0,2	0,5	-
Evaluation	100%	3,6	3,7	**4,6**	3,5	-

The evaluation highlights clear differences between the printing strategies. The axial MA-FFF method receives the lowest rating of 3.5 points, as the improved mechanical properties are not relevant for this component. The Inclined Layer Printing (ILP) strategy and the 3A-FFF method score similarly, with ratings of 3.7 and 3.6 points, respectively. Both are suitable for producing high-quality parts but have specific drawbacks. The MA-FFF strategy for curved structures achieves the highest rating of 4.6 points, offering the best combination of part quality and production costs, making it the optimal choice for this component.

The demonstrator component was printed and evaluated using both the 3A-FFF and MA-FFF methods to assess the practical applicability of the DC. In the 3A-FFF process, the part quality exceeded expectations, though challenges such as the stair-stepping effect and poor surface finish due to support material were encountered. The evaluation of part quality was slightly improved. In the MA-FFF process, the part quality met high expectations and was rated 5.

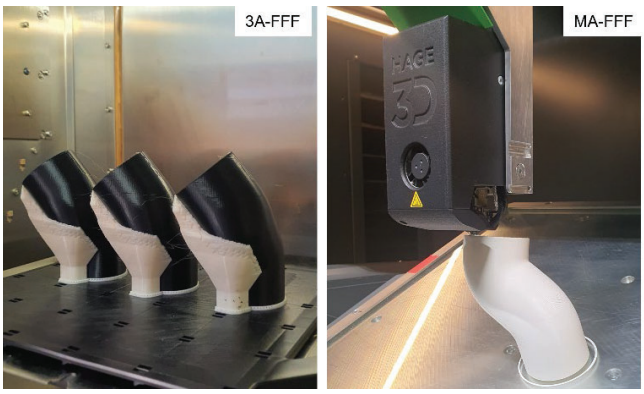

Fig. 2. Manufactured components.

IV. Conclusions

The practical implementation and evaluation of the components using both the 3A-FFF and MA-FFF methods demonstrates that the theoretical inputs and ratings were largely confirmed. Minor deviations between theoretical assumptions and actual results were observed, but these had only a minimal impact on the overall assessment. These deviations are attributed to the fact that the original ratings were based on experiential values. With increasing user experience, results become more precise, leading to more accurate evaluations. The practical printing results confirm the theoretical evaluations of the DC. The developed DC represents a robust and methodologically sound tool for evaluating and selecting FFF printing methods.

REFERENCES

[1] Berger, U., Hartmann, A. u. Schmid, D.: 3D-Druck - additive Fertigungsverfahren. Rapid Prototyping, Rapid Tooling, Rapid Manufacturing. Europa Lehrmittel. Haan-Gruiten: Verlag Europa-Lehrmittel Nourney, Vollmer GmbH & Co. KG, 2019

[2] Roy, S.: Embracing the Future: How Space Organizations are Integrating Additive Manufacturing Technologies, 2023

[3] Kubalak, J. R., Wicks, A. L. u. Williams, C. B.: Exploring multi-axis material extrusion additive manufacturing for improving mechanical properties of printed parts. Rapid Prototyping Journal 25, pp. 356–362, 2019.

[4] Brandstötter, M., Petersmann, S. u. Bosch, J.: Roboterbasierter 3D-Druck mit neuen Dimensionen. e & i Elektrotechnik und Informationstechnik 140, pp. 536–540, 2023

[5] Zhao, D. u. Guo, W.: Mixed-layer adaptive slicing for robotic Additive Manufacturing (AM) based on decomposing and regrouping. Journal of Intelligent Manufacturing 31, pp. 985–1002, 2021

[6] Chakraborty, D., Aneesh Reddy, B. u. Roy Choudhury, A.: Extruder path generation for Curved Layer Fused Deposition Modeling. Computer-Aided Design 40, pp. 235–243, 2008

[7] Solomon, I. J., Sevvel, P. u. Gunasekaran, J.: A review on the various processing parameters in FDM. Materials Today: Proceedings 37 (2021), S. 509–514

[8] Buj-Corral, I., Domínguez-Fernández, A. u. Durán-Llucià, R.: Influence of Print Orientation on Surface Roughness in Fused Deposition Modeling (FDM) Processes. Materials 12 (2019) 23, S. 3834

[9] Leoni, A., Stornelli, V. u. Pantoli, L.: Print On Air: FDM 3D Printing Without Supports. Sensors and Actuators A: Physical 280 (2018), S. 543–551

[10] VDI Verein Deutscher Ingenieure: Additive Fertigungsverfahren Grundlagen, Begriffe, Verfahrensbeschreibungen (2014) VDI 3405

[11] Rajaguru, K., Karthikeyan, T. u. Vijayan, V.: Additive manufacturing – State of art. Materials Today: Proceedings 21 (2020), S. 628–633

[12] VDI Verein Deutscher Ingenieure: Additive Fertigungsverfahren Gestalungsempfelung für die Bauteilfertigung mit Materialextusionsverfahren (2021) VDI 3405 Blatt 3.4

[13] Zhang, B., Goel, A., Ghalsasi, O. u. Anand, S.: CAD-based design and pre-processing tools for additive manufacturing. Journal of Manufacturing Systems 52 (2019), S. 227–241

[14] Kumbhar, N. N. u. Mulay, A. V.: Post Processing Methods used to Improve Surface Finish of Products which are Manufactured by Additive Manufacturing Technologies: A Review. Journal of The Institution of Engineers (India): Series C 99 (2018) 4, S. 481–487

[15] Miguel Fernandez-Vicente, Miquel Canyada, Andres Conejero: Identifying limitations for design for manufacturing with desktop FFF 3D printers. Rapid Manufacturing, (2015)

[16] Leary, M., Babaee, M., Brandt, M. u. Subic, A.: Feasible Build Orientations for Self-Supporting Fused Deposition Manufacture: A Novel Approach to Space-Filling Tesselated Geometries. Advanced Materials Research 633 (2013), S. 148–168

[17] Müller, J.: Arbeitsmethoden der Technikwissenschaften: Systematik, Heuristik, Kreativität. Springer, Berlin (1990)

Comparative Study of Additive Silicone Manufacturing Methods for Medical Devices

Sebastian Lämmermann[1]*, Martin Reiter[1], Zoltan Major[1]

Institute of Polymer Product Engineering, Johannes Kepler University Linz, Austria[1]

Corresponding Author: sebastian.laemmermann@jku.at*

Abstract—**This study evaluates different methods for fabricating silicone elastomers, comparing conventional mould casting with direct and gel-supported 3D printing. Standardized specimens made from Sylgard 184 were tested for mechanical properties and dimensional accuracy. Results show that cast parts generally exhibit superior strength and precision, although air entrapment can compromise quality. In contrast, 3D printing enables more complex geometries but remains limited in performance.**

I. Introduction

Since additive manufacturing became widely available to the broader public, it profoundly changed many areas of manufacturing. One of the biggest impacts has been in personalized healthcare. Here the main materials used are metal alloys, thermoplastic polymers and UV-curable resins. In addition, silicone elastomers play a major role in healthcare. However, despite extensive research efforts [1], only a small number of commercially available printer systems exist today.

An early system for silicone 3D printing was developed by GermanReprap (now part of innovatiQ [2]), which employed a heat source to cure a two-component silicone. Subsequent iterations introduced a second printhead for support material, enabling the fabrication of more complex geometries.

Another approach resembles the freeform reversible embedding method described by Hinton et al. [3], in which the printed silicone is deposited into a support gel that counteracts gravitational deformation. This enables the fabrication of complex parts without additional support structures. After printing, the part can be cured either by heating the entire medium or by allowing the silicone to cure at ambient conditions. A commercial implementation of this technique is offered by Rapid Liquid Printing [4].

This study evaluates these silicone 3D-printing methods and compares them with the traditional rapid tooling approach of printing a mould from thermoplastic material and casting the silicone part within it.

II. Methodology

To ensure comparability with existing literature, all specimens were fabricated using the widely available silicone elastomer Sylgard 184 (Dow Chemical, Midland, US). Prior to processing, the two components were thoroughly mixed in a container of suitable size and subsequently degassed for 5 min to remove entrapped air. The prepared material was then transferred into syringes equipped with Luer-Lock adapters and used either for direct printing or for casting the test specimens. For the evaluation of mechanical properties, standardized ISO tensile specimens were produced, while printing parameters were additionally investigated by fabricating dome-shaped structures to assess accuracy and resolution.

Casting moulds were additively manufactured from PLA using a Prusa XL (Prusa Research, Czech Republic) equipped with a 0.4 mm nozzle and the default print settings provided in PrusaSlicer 2.9.2. After printing, the moulds were coated with two layers of mould release agent. The silicone was injected using a syringe actuated by a pneumatic piston. The filled moulds were then left to cure under ambient conditions for 72 h before demoulding.

All silicone structures intended for printing were prepared using PrusaSlicer 2.9.2, with a fixed layer height of 0.2 mm, a single perimeter, and 100% rectilinear infill. The printing speed was set to 20 mm/s. For direct silicone printing, a core-XY 3D printer frame was equipped with a vipro-HEAD 3/3 endless piston extrusion head (Viscotec, Germany). Layer curing by heat and infrared radiation was achieved using a 1.5 kW halogen lamp mounted on the rear of the x-axis and positioned 20 mm above the nozzle tip. The material was deposited onto a glass build platform through a 0.4 mm blunt Luer-Lock needle.

For gel-supported printing, the hydrogel support medium was prepared following literature procedures [3]. A total of 6 g of Carbopol 940 (Lubrizol, United States) was dispersed in 500 mL of water, thoroughly mixed, and repeatedly degassed. The dispersion was then mixed with 5 mL of 1M NaOH to initiate gelation. After storage at 4 °C for at least 24 h, the gel was transferred into a suitable container for use as a support bath. The deposited silicone cured gradually at room temperature, after which the solidified component was carefully extracted from the gel.

All printed and cast specimens were mechanically characterized using a uniaxial servo-hydraulic testing system operated at a piston speed of 50 mm/min. Dimensional resolution and geometric accuracy of the fabricated samples were further analysed using computed tomography (CT) scanning.

III. Results

Test specimens and sample components were successfully fabricated using all three investigated strategies. Casting of the specimens and components was achieved reliably with the described technique. Figure 1 illustrates the opened mould containing the tensile specimens. The mould cavities filled completely, with only a small amount of flashing observed between the mould halves. For cast specimens, mould design was a crucial factor, as even minor air entrapments could lead to optical imperfections and initiate mechanical defects within the manufactured parts. Furthermore, particular care was required during degassing and injection of the material into the mould to minimize the risk of void formation.

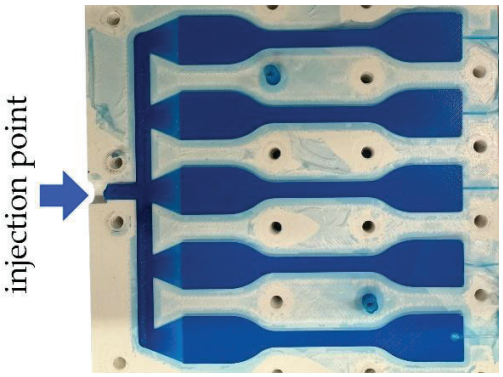

Fig 1: Opened mould with cast tensile specimens

Direct printing of silicone was also successfully accomplished. However, both direct printing and gel-supported printing posed distinct challenges. For direct printing with infrared-assisted curing (Fig. 2a), the exposure time had to be adapted carefully to the geometry of the printed part. If the exposure time was too short, the deposited silicone remained soft and was unable to support subsequent layers, whereas excessively long exposure times resulted in thermal degradation of the material.

Gel-supported printing also produced parts successfully as shown in Figure 2b. The key parameter was extrusion rate. Insufficient extrusion reduced connectivity, while excessive extrusion caused visible surface defects and distortions.

Mechanical testing revealed that both cast and directly printed specimens exhibited excellent mechanical properties with comparable performance. In terms of dimensional resolution and surface quality, casting achieved the highest fidelity, as the resolution was limited only by the accuracy of the mould. In contrast, direct printing produced smoother but less sharply defined geometric features due to the low viscosity of the silicone and the compliance of the surrounding gel.

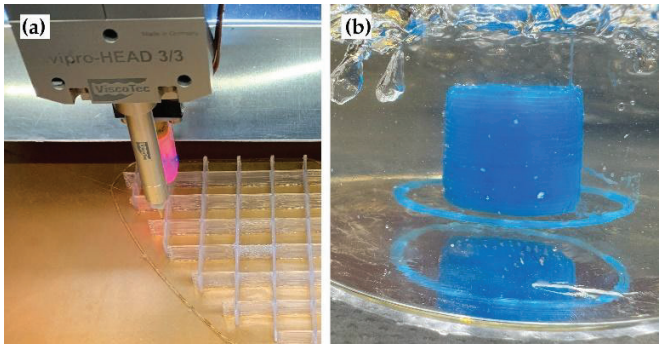

Fig. 2: (a) Direct additive manufacturing of a silicone structure using IR curing, (b) Silicone structure suspended in gel support bath

IV. Conclusions

All three investigated methods proved to be viable processes for producing silicone components for medical applications.

Casting generally achieved the highest resolution and geometric accuracy, as the fidelity of the final component directly reflected the precision of the mould. However, the design and fabrication of moulds can become particularly complex for medical applications, especially when freeform geometries are required. While highly accurate, this complexity limits the practicality of casting for individualized or intricate medical parts.

In contrast, direct and gel-supported 3D printing offer greater design flexibility, enabling the fabrication of complex or patient-specific geometries without the need for elaborate moulds. Gel-supported printing, in particular, provides stability for freeform structures that cannot be realized through direct extrusion alone.

Future work should focus on optimizing printing parameters, improving curing strategies, and expanding the material palette to further close the performance gap between printed and cast silicone components.

V. Acknowledgements

This work has been supported by the Johannes Kepler University Linz via the Lift-C CETUS Project.

VI. References

[1] Liravi, Farzad; Toyserkani, Ehsan (2018): Additive manufacturing of silicone structures: A review and prospective. In: Additive Manufacturing 24, S. 232–242. DOI: 10.1016/j.addma.2018.10.002.

[2] innovatiQ GmbH | LAM SILIKONDRUCKER LiQ 5 (2025). Available from https://www.innovatiq.com/drucker/liq5, Accessed 05.09.2025.

[3] Hinton, Thomas J.; Hudson, Andrew; Pusch, Kira; Lee, Andrew; Feinberg, Adam W. (2016): 3D Printing PDMS Elastomer in a Hydrophilic Support Bath via Freeform Reversible Embedding. In: ACS biomaterials science & engineering 2 (10), S. 1781–1786. DOI: 10.1021/acsbiomaterials.6b00170.

[4] Rapid Liquid Print Co. (2025): Technology. Available from https://www.rapidliquidprint.com/, Accessed 12.09.2025.

Towards full-field thermal monitoring during additive manufacturing process using simulation- & ML-based virtual sensing

Monika Stipsitz[1]*, Hèlios Sanchis-Alepuz[1]

Embedded Systems
Silicon Austria Labs GmbH, Graz, Austria[1]
Corresponding Author: monika.stipsitz@silicon-austria.com*

***Abstract*—The temperature distribution within a sample during the manufacturing process is a key factor influencing the final sample quality, and would, thus, be an invaluable input for process control. In this work, we investigate if ML-based virtual sensing combined with physics-based simulations can be a useful tool for reconstructing the full temperature distribution within a sample with sufficient accuracy and speed to enable real-time monitoring during the print process. We present a novel approach to design a training dataset based on randomized geometries, and show that a neural network trained on this data generalizes well to variable and previously unseen geometries. We evaluate the approach for the standard calibration cube at various intermediate printing states and environment conditions. The high predictive accuracy obtained on the randomized dataset suggest a realistic path towards real-time monitoring.**

I. Introduction

Accurate knowledge of the temperature distribution within a sample during additive manufacturing (AM) is essential for controlling the final print quality. Traditional monitoring approaches rely on high-fidelity physics-based simulations, such as finite element methods [1]. While accurate, these simulations are computationally intensive and difficult to scale for real-time process control. Also, they require unrealistically detailed knowledge of the system (boundary conditions, latent heat distribution, etc.). Experimental alternatives like infrared thermography and pyrometry provide surface-level temperature data but cannot capture internal thermal histories [2], and are costly. To address these limitations, recent research has explored data-driven surrogate models (including neural networks [3] and Gaussian processes [4]) trained on simulation or experimental data to enable rapid thermal predictions. However, these models often lack robustness across varying geometries and process parameters. Emerging physics-informed machine learning methods, such as Physics-Informed Neural Networks (PINNs), offer a hybrid approach by embedding physical laws into learning frameworks, improving generalization and physical consistency [5], [6]. However, if the underlying PDEs are only approximate models (which is often the case in AM due to simplifications like constant material properties or ignoring latent heat), then enforcing them strictly during training can lead to biased or incorrect predictions. Also, PINNs struggle with handling irregular or evolving geometries (like a growing melt pool).

In this work, we investigate a physics-based machine learning approach that leverages data from physics-based simulations and combines it with (in this preliminary study, artificial) measurement data to infer the internal temperature distribution in a manufactured part during the build process. To ensure generalization to different (growing) geometries, we employ a novel strategy for designing random geometries for model training. We present first results of this ongoing research, which demonstrate high predictive accuracy, suggesting a viable path forward for real-time, non-intrusive thermal monitoring during the AM process.

II. Approach

(1) Modelling of AM process: To generate synthetic training data for the temperature field prediction task, we employ a simplified finite element (FE) simulation model that captures key aspects of the additive manufacturing process. At each discrete time step, a cubic volume element (side length $a = 0.4\,\mathrm{mm}$) representing newly deposited material is added to the domain. A fixed heat input, denoted by $h_{\max}$, is applied locally to the newly added cube to mimic the deposition of hot material. Material elements deposited in previous time steps retain a fraction α of their previous heat input, reflecting the decrease of heat contribution over time. The FE model solves the transient heat equation over the evolving geometry, and records the resulting 3D temperature distribution at each time step. For simplicity, we use plastic material properties in this study, however, we have previously proven for electronic system monitoring

that our approach is feasible for highly-conductive and mixed materials as well [7].

For this initial study, the approach is evaluated for the standard calibration cube. For ease of transferring the data from the FEM simulation to the employed ML model, we rasterize the test geometry (see Fig. 1). The rasterized model is obtained from the gcode of the system using a custom python script to transfer the print path to the scriptable CAD tool `FreeCAD`. While this rasterization limits the application to real-world geometries, it is not strictly necessary for our approach, and will be lifted in future work.

We conduct transient FE simulations using the open-source FE solver `Elmer`. The boundary conditions (BC) consist of a Dirichlet BC at the bottom of the system representing a constant bed temperature T_{bed}, and Robin BCs with a constant ambient temperature T_{amb} and heat transfer coefficient α_{air} representing convective cooling on all outer surfaces of the system. Note, that for simplicity convective cooling uses constant parameters (T_{amb}, α_{air}) on all the outer surfaces. However, the simulations are set up in a versatile way, such that this restriction will be lifted in future work.

These types of FEM simulations are used for the evaluation of our approach. To represent variable conditions during manufacturing, we conduct a series of simulations with variable values for the chamber temperature T_{amb}, heat transfer coefficient α_{air} representing convective cooling, heat source introduced via the nozzle h_{max}, cooling rate α, and bed temperature T_{bed}.

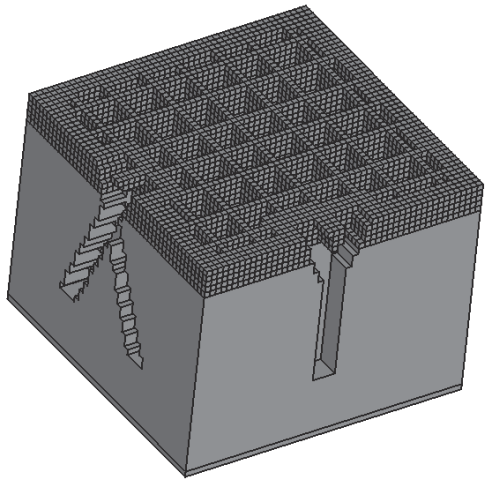

Fig. 1. Illustration of an intermediate rasterized geometries of the calibration cube.

(2) Design of training dataset: In principle, one could compose a training dataset by generating a large number of simulations as described in the previous paragraph – for each simulation varying the deposition sequence and spatial pattern of added cubes. However, we have seen in previous projects [8] that this direct approach is very inefficient and the dataset lacks the variability necessary to accurately generalize to a wide range of unseen geometries. Instead, we construct a set of random geometries by randomly placing cubes with side length $a = 0.4\,\text{mm}$ on a baseplate (a detailed description of how these systems are build and prepared for FE simulations using open-source tools can be found in [8]).

(3) Physics-based ML model: In this study, we train a fully-convolutional neural network (NN) to estimate the temperature distribution within the 3D geometry with a resolution of 0.4 mm (see Fig. 2 for an overview of the training approach). We train the network to reproduce the temperature distribution within the sample at any given time instance t_i. In this first version, we investigate only a basic temperature monitoring scenario, where we assume only the geometry and nozzle / bed temperature are known. Thus, we use only geometrical / material information and estimated heat distributions as input to the NN. Thus, the inputs are the geometry at a given time instance t_i, the estimated heat source distribution at t_i based on the print path until t_i (as described in paragraph (1)), and the predicted full-field temperature distribution for times $t < t_i$.

In future work, we plan to investigate how the reconstruction can be improved to better replicate more realistic scenarios with unknown environment conditions given additional sensory information as input, e.g. basic sensor information like temperature measurements of the ambient / chamber temperature or more advanced setups including the surface temperature as obtained from a thermal camera.

III. Preliminary Results & Discussion

The NNs are trained using a 80 % : 20 % train-test split of the training dataset. The training loss consists of a normalized L_1-loss combined with a physics-based loss L_H as a regularizer:

$$L = L_1 + \lambda L_H. \tag{1}$$

L_H is derived from an integral formulation of the discretized transient heat equation similar to the one applied in [8]. Note, that in contrast to PINNs, the NN training is not predominantly driven by the simplified partial differential equation, but the physics-based loss term L_H is used as a regularizer (with $\lambda = 10^{-4}$) to improve generalizability. After training, the NN is evaluated for the standard calibration cube at various intermediate printing states and environment conditions.

The mean L_1 error for the one-step prediction on the test partition of the randomized dataset was below 0.1 %, and maximum mean error below 4 %. Preliminary results on the evaluation for the rasterized 3D printing geometry suggest that errors below 10 % can be reasonably achieved. The fully convolusional structure of the NN assures a reasonably small number of parameters (less

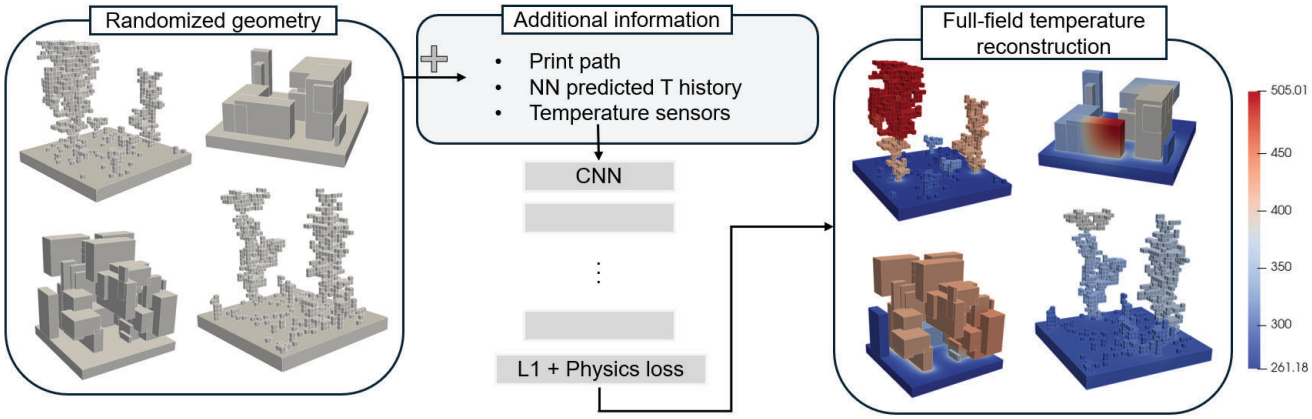

Fig. 2. Overview of the training approach: A multi-layer fully convolutional NN (CNN) is trained based on a dataset of randomly distributed blocks and heat sources (see left side) to reconstruct the temperature distributions from FE simulations (right side). The colors in the temperature reconstructions represent temperature in K (see scale on the right). The training is driven by a combination of the normalized mean error per system (L_1 loss) combined with a physics-based regularization term.

than 10 million parameters). On a high-end GPU (on one out of 18 identical shards of an NVIDIA A100 80GB PCIe GPU with CUDA Version 12.4) the model achieves an inference time of approximately 3 milliseconds [7] without dedicated model optimization. The model is, thus, well suited (after proper optimization) to be employed for real-time monitoring.

Future work will focus on systematically investigating the influence of available sensor data on the reconstruction quality, particularly under realistic and resource-constrained conditions typical of industrial 3D AM setups. To validate the proposed approach, we plan to conduct controlled laboratory experiments with thermal imaging and embedded temperature sensors to benchmark the virtual sensing predictions against ground truth. In parallel, improvements to the geometry rasterization pipeline are essential to enable high-fidelity reconstructions for complex, nontrivial part geometries commonly encountered in practical AM applications. Lastly, we aim to generalize the framework to support multi-material processes.

Acknowledgement

This work has been supported by Silicon Austria Labs (SAL), owned by the Republic of Austria, the Styrian Business Promotion Agency (SFG), the federal state of Carinthia, the Upper Austrian Research (UAR), and the Austrian Association for the Electric and Electronics Industry (FEEI).

References

[1] Z. Luo and Y. Zhao, "A survey of finite element analysis of temperature and thermal stress fields in powder bed fusion additive manufacturing," *Additive Manufacturing*, vol. 21, pp. 318–332, 5 2018.

[2] L. Chen, G. Bi, X. Yao, J. Su, C. Tan, W. Feng, M. Benakis, Y. Chew, and S. K. Moon, "In-situ process monitoring and adaptive quality enhancement in laser additive manufacturing: a critical review," *Journal of Manufacturing Systems*, vol. 74, pp. 527–574, 4 2024.

[3] W. Jiao, D. Zhao, S. Yang, X. Xu, X. Zhang, L. Li, and H. Chen, "Real-time prediction of temperature field during welding by data-mechanism driving," *Journal of Manufacturing Processes*, vol. 133, pp. 260–270, 1 2025.

[4] X. Li and N. Polydorides, "Time-efficient surrogate models of thermal modeling in laser powder bed fusion," *Additive Manufacturing*, vol. 59, p. 103122, 11 2022.

[5] S. Li, G. Wang, Y. Di, L. Wang, H. Wang, and Q. Zhou, "A physics-informed neural network framework to predict 3d temperature field without labeled data in process of laser metal deposition," *Engineering Applications of Artificial Intelligence*, vol. 120, p. 105908, 4 2023.

[6] B. Peng and A. Panesar, "Multi-layer thermal simulation using physics-informed neural network," *Additive Manufacturing*, vol. 95, p. 104498, 9 2024.

[7] S. Sabathiel, H. Sanchis-Alepuz, A. S. Wilson, J. Reynvaan, and M. Stipsitz, "Neural network-based reconstruction of steady-state temperature systems with unknown material composition," *Scientific Reports 2024 14:1*, vol. 14, pp. 1–12, 9 2024. [Online]. Available: https://www.nature.com/articles/s41598-024-73380-1

[8] M. Stipsitz and H. Sanchis-Alepuz, "Approximating the full-field temperature evolution in 3d electronic systems from randomized "minecraft" systems," in *8th European Congress on Computational Methods in Applied Sciences and Engineering*. CIMNE, 2022. [Online]. Available: https://www.scipedia.com/public/Stipsitz_Sanchis-Alepuz_2022a

functionalWOOD2print – Binder-jet 3D printing of tough biobased structural materials with functional surfaces

Doris Kapl[1]*, Katrin Fradler[1], Christoph Jocham[1], Jürgen Leßlhumer[2], Thomas Steiner[3]

Kompetenzzentrum Holz GmbH, Smart Composites & Surfaces,
St. Veit an der Glan, Austria[1]
Kompetenzzentrum Holz GmbH, Biobased Composites,
Applications & Processes, Linz, Austria[2]
Haratech GmbH, Linz, Austria[3]
*Corresponding Author: d.kapl@wood-kplus.at**

I. Introduction

Additive manufacturing (AM) significantly expands the freedom of design and individualization of components and assemblies in comparison to conventional processes [1]. However, there is a lack of technically and industrially usable AM processes for the production of tough materials made of wood and biobased raw materials that are available in large quantities from by-products of the wood and paper processing industry. Powder bed-based AM processes could close this gap with the binder jetting technology (BJ3DP). During the binder-jetting process, a powder based raw material is applied layer by layer and connected at selected areas by means of a binder [2]. Thus, binder jetting processes proceed at low temperatures which is crucial to circumvent degradation of wood fibers as a result of high energy input. Moreover, binder jetting is very well suited for industrial production due to large build spaces, high build rates and, above all, no support structures are required that must be removed as production waste. Another advantage of the binder jetting process is the possibility to use different binders applied via the print head. Thus, various mechanical and decorative properties can be achieved [3].

BJ3DP is already in widespread use for pure and gypsum-filled polymers as well as for green body production of metal sintered parts [4]. However, bio-based BJ3DP systems producing a bio-based material matrix, reinforcing fibers and fillers as well as binders have hardly been described in scientific literature so far and are missing on the market as designated process raw materials [5,6]. There is also a lack of bio-based infiltration resins which are used after removal of the component from the powder bed to close open porosity and increase mechanical properties. Thus, this work focuses on the material selection of biobased powders that can be used in the binder jetting process as well as suitable binders and infiltration resins.

II. Material selection

The material selection requires thorough screening of powders which can be processed in the 3D-printer and deliver the desired properties to the printed part. Characteristics such as flowability, bulk density, particle size distribution, and optical properties highly impact the processability. In this work, biobased powders, namely wood, cellulose and lignin powders of different particle sizes and modifications were considered as raw materials. Moreover, additives were investigated to improve the flowability or mechanical properties of the printed parts.

The selection of the binder system opens up two possibilities. The first one is the application of a liquid binder which is applied via the printer nozzle to the powder bed. This method has the advantage of generating a denser product but brings the risk of clogging the printer nozzles. Moreover, only low viscous liquids can be used, which is a severe restriction to a wide range of biobased adhesives. The second possibility is the use of a powder binder which is mixed with the biobased raw material. Upon addition of a liquid via the printer nozzle this powder binder dissolves and adheres the powder particles upon drying. This method allows a wide range of binders and is especially interesting with regard to biobased materials where the viscosity is a limiting factor [3].

Selection of suitable infiltration resins is also required since the 3D printing process generates a green part with high porosity. In order to increase the density an infiltration process is inevitable. Important parameters of infiltration resins are low viscosity (<600 mPa.S) to achieve full permeation of the printed part, relatively low curing temperatures (<120 °C) to circumvent degradation of the biobased materials, the color, and the mechanical properties which are delivered to the final 3D printed part.

III. Methodology

For the preselection of suitable powders and powder mixtures, the flowabilities and particle sizes were

investigated. Then, printing trials were performed with a ProJet 660Pro 3D-printer from 3D SYSTEMS. During these experiments the behavior during layer and binder application was investigated. Based on these experiments two powders, namely a microcrystalline cellulose and a very fine wood powder were selected for further experiments.

In the next step, liquid as well as powder binders were investigated. For the development of a liquid binder, solutions of water-soluble polymers such as polyvinyl pyrrolidone (PVP) and polyvinyl alcohol (PVA) as well as a water/glycerine/isopropanol mixture were prepared, and a surfactant was added to decrease the surface tension. Relevant properties such as dynamic viscosity, density, and surface tension were determined. Finally, an aqueous formulation based on PVP was developed which conforms in relevant parameters to the liquid binder commercially used in the printer system. This formulation was further used for contact angle measurements on the powder bed to investigate the interaction of the liquid binder with the powder during application [7].

For further testing of liquid binders and for the selection of powder binders an out-of printer screening method was established [8]. Thereby, the powder was mixed with the binder in a beaker. The resulting slurry was filled into cylindrical molds and left to dry at room temperature. The fabricated test specimens were investigated with respect to shrinkage, deformation, color, and compressive strength. Best results were obtained with PVP applied as powder binder (Figure 1). In further trials the concentration impact was studied. Moreover, this method was used to investigate if the addition of nanocellulose has a reinforcing effect on the printed material.

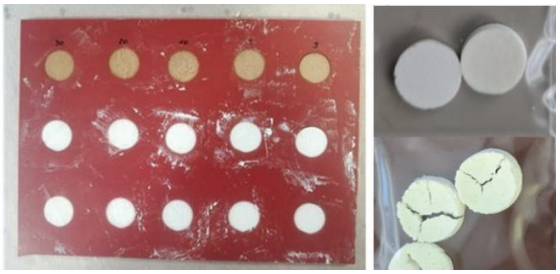

Fig. 1. Screening method for powder and binder selection. Powder/binder mixtures were filled into cylindrical molds (left) and dried at RT. Resulting test specimens (top: with PVP binder, bottom: with hydroxyethyl cellulose binder) were further characterized.

After the screening process, 3D binder jetting trials were performed. These experiments showed that the selected powder/binder mixture can be processed in the printer and first green parts could be obtained (Figure 2). However, further adaptations of the printer software and hardware are required to fully exploit the possibilities of the selected materials.

Fig. 2. Green part obtained by 3D binder jetting trials with the selected microcrystalline cellulose powder with PVP applied as powder binder.

After the 3D printing process, a green part with high porosity is obtained. In order to increase the density, post-processing is crucial. Therefore, commercially available resins, such as an epoxide resin, lauryl methacrylate (LM), and isobornyl methacrylate (IBOMA), having a biobased content of 29%, 70%, and 72% respectively were tested. Differential scanning calorimetry (DSC) was conducted to examine the curing behavior, and model-free kinetics were employed for the analysis. Then, test bodies which were obtained by the binder screening method described above were inserted into the infiltration resin. After curing, the test specimens were again examined with respect to color, shrinkage, deformation, and compressive strength. These experiments demonstrated that the infiltration process, especially the epoxide resin, is able to increase the mechanical properties significantly. However, the epoxide resin leads to a yellow color stain which is not the case when IBOMA is used.

IV. Conclusions and Future Work

During this work, a screening method was established to select possible raw materials and binders for the binder jetting process based on biobased materials. Moreover, first printing trials were performed, and different infiltration resins were tested. Further work includes the evaluation of further materials and fine tuning of powder and binder mixtures as well as infiltration resins. Moreover, the adaptation of the 3D printer soft- and hardware plays a central role for better adjustment of the parameters to the biobased raw materials.

Acknowledgement

This project is funded by the Walfonds fund, an initiative of the Federal Ministry of Agriculture, Forestry, Regions, and Water Management, and is carried out as part of the Think.Wood program of the Austrian Wood Initiative.

Waldfonds
Republik Österreich
Eine Initiative des Bundesministeriums für Land- und Forstwirtschaft, Regionen und Wasserwirtschaft
https://www.waldfonds.at/

FFG
Forschung wirkt.
https://www.ffg.at/programm/thinkwood

REFERENCES

[1] A. Bhatia, A. K. Sehgal, "Additive manufacturing materials, methods and applications: A review", *Materials Today: Proceedings*, vol. 81, p. 1060-1067, 2023.

[2] A. K. Das, D. A Agar, M. Rudolfsson, S. H. Larsson, "A review on wood powders in 3D printing: processes, properties and potential applications", *Journal of Materials Research and Technology*, vol 15, p. 241-255, 2021

[3] M. Ziaee, N. B. Crane, "Binder Jetting: A Review of Process, Materials, and Methods", *Additive Manufacturing*, 2019.

[4] A. Mostafaei, A. M. Elliot, J. E. Barnes, F. Li, W. Tan, C. L. Cramer, P. Nandwana, M. Chmielus, "Binder jet 3D printing – Process parameters, materials properties, modeling, and challenges", *Progress in Materials Science*, vol 119, P 100707, 2021

[5] H. Zeidler, D. Klemm, F. Böttger-Hiller, S. Fritsch, M.J. L. Guen, S. Singamneni, "3D printing of biodegradable parts using renewable biobased materials", *Procedia Manufacturing*, vol. 21, p. 117-124, 2018.

[6] F. Dini, S. A. Ghaffari, J. Javadpour, H. R. Rezaie, "Binder Jetting of hydroxyapatite/Carboxymethyl Chitosan/polyvinyl pyrrolidone/Dextrin Composite: The role of Polymeric Adhesive and Particle Size Distribution on Printability of Powders", *JMEPEG*, vol. 31. P. 5801-5811, 2022.

[7] W. Chai, Q. Wei, M. Yang, K. Ji, Y. Guo, S. Wei, Y. Wang, "The pintability of three water based polymeric binders and their effects on the properties of 3D printed hydroxyapatite bone scaffold", *Ceramics International*, vol 46, p. 6663-6671, 2020.

[8] S. I. Yanez-Sanchez, M. D. Lennox, D. Therriault, B. D. Favis, J. R. Tavares, "Model Approach for Binder Selection in Binder Jetting", *Industrial & Engineering Chemistry Research*, vol. 60, p. 15162-15173, 2021.

Sustainability in Additive Manufacturing - Influence of Powder Reuse on High Temperature Strength in L-PBF of Ti6Al4V

Benjamin Meier-Leeb[1]* and Fernando Warchomicka[2]

Department Engineering and IT, Carinthia University of Applied Science, Villach, Austria[1]
IMAT Institute of Material Science, Joining and Forming, Graz University of Technology, Graz, Austria[2]
Corresponding Author: b.meier-leeb@fh-kaernten.at*

Abstract— **Effects of the reuse of powder within the Laser Powder Bed Fusion process is one of the crucial questions for the ecological and economical sustainability of this additive manufacturing technology. This is especially the case for critical structural components and reactive materials like titanium alloy Ti6Al4V, which tends to pick up elements like Oxygen and Hydrogen leading to increased brittleness and porosity.**

However, the increase in oxygen stabilizes the alpha phase in titanium alloys, which is preferred for high temperature application as it is more resistant to hydrogen and oxygen pick up at higher temperatures than the beta phase.

In the scope if this work the influence of the changing materials properties of Ti6Al4V, caused by powder reuse within the L-PBF process, on the high temperature tensile strength are investigated.

I. Introduction

Ti6Al4V Grade 5 (Ti64) is the most widely used titanium alloy and is well established in additive manufacturing, especially Laser Powder Bed Fusion (L-PBF). However, the L-PBF process requires large amounts of powder to fill the bed around the manufactured components, affecting the environmental footprint and its economic competitiveness. Therefore, the powder has to be reused several times to achieve a materials usage rate of over 90% from powder to finished product, compared to subtractive methods where, up to 95% of the material ends up as scrap, as shown by Paris et al. [1], Morrow et al. [2] and Huang et al. [3].

This reuse procedure affects the material properties, however the measured impact varies in different studies. An overview of the results is given in Meier et al. [4], with a common finding of increasing oxygen levels.

Especially in aerospace applications, such as gas turbine engines and adjected components, the strength of Ti64 at elevated temperature is of high interest since its density is nearly half of the otherwise used high-temperature resistant Ni-Superalloys [6][7]. For classically wrought, forged, and machined Ti64, the maximal service temperature is limited by the poor oxidation resistance at temperatures higher than 400°C. An increased oxygen intake leads to the formation of α case, loss in ductility and fatigue strength [6][7]. Therefore, the MMPDS standard suggests its use up to 400°C [8], as do Lütjering and Williams [7].

Ti64 processed by L-PBF establishes a non-equilibrium martensitic microstructure, which is more resistant to α case formation than equilibrium $\alpha + \beta$ microstructure [7]. While more brittle at room temperature it shows high strength combined with sufficient ductility at elevated temperatures [9]. Recently Viespoli et al. [10] investigated the fatigue and creep strength of as-build, martensitic Ti64 samples at temperatures up to 600°C. While fatigue samples suffered from the surface defects also found in previous work on fatigue at room temperature [11][12], the impact of an ambient temperature was comparable to conventional processed materials [8]. Also the creep strength was foun do be similar by Viespoli et al. [10].

Xie et al. [13] investigated fracture toughness, fatigue and tensile strength of the $\alpha + \beta$ alloy Ti6Al3Mo1Zr, with optimized heat treatments. Other research groups also investigate the properties of the near α Titanium Alloys Ti–6.5Al–2Zr–1Mo–1V [14][15] and Ti6Al2Sn4Zr2Mo [16] conventionally used for high temperature application [6][7], as well as the metastable β alloy Ti-17 [17], known for improved fatigue properties. Though they exhibit excellent [14] [15] and promising [16] high temperature (tensile) properties the processing (and heat treatment) itself is a lot more challenging than for Ti64 [18][19].

Based on the work done in [4] and [9] this paper investigates the effect of reusing powder and the resulting changes in chemical composition on the high temperature tensile strength of the material.

II. METHODOLOGY

The methods applied for testing align with those found in in the previous work leading to this study [4][9]. Samples were produced on an EOS M280 L-PBF machine, with powder being reused 18 times in a single batch regime, under continuous control of the powder (chemical composition and rheology) and bulk material properties (density, tensile and Charpy strength). Of these jobs, 15 reached an sufficient high to deliver useable vertical test samples. High temperature tensile tests were performed on an Gleeble 3800, with an adapted shortened specimen design shown in Figure 1a. This design ought to reduce the temperature gradient due to the direct resistance heating system in the Gleeble machine and by the overall reduced sample length allow for vertical samples over a higher number of reuse cycles [4]. Additionally, the design was optimized (notches) to use a Gleeble specific extensometer (C-gauge) system. For temperature control thermocouples were welded to the center of the gauge length, and for selected samples at one or both end of the gauge length to measure the temperature gradient.

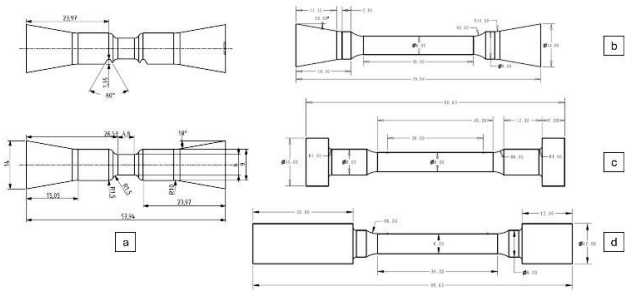

Fig. 1. Test specimen design for tensile test. a) shortened Gleeble 3800 specimen, b) long specimen for Gleeble with gauge length according to ASTM E8, c) ASTM E8 specimen for Zwick Roll, and d) ASTM 21 specimens for Instron machine

Test were performed at room temperature, 120°C and 400°C for stress relieved (SR) and furnace annealed (FA) samples, for virgin powder and after 4, 6, 8, 10, 12, 13, 14, and 15 reuse cycles. The number of successfully tested samples for can be found in the test matrix (Table 1). For virgin powder test shortened (Fig 1a), standard ASTM E8/21 (Fig 1c & d), and ASTM E8 based specimen modified for Gleeble clamping (Fig. 1b) were performed to ensure comparability. Based on the measured temperature gradients in the previous work [9] short specimen geometry was used for tests at 400°C while the long samples were used at 120°C.

Tab. 1. Experimental matrix

Reuse Cycles	Temperature	Specimen and Heat Treatment					
		Gleeble Short		Gleeble Long		ASTM E8/E21	
		SR	FA	SR	FA	SR	FA
Virgin	RT			2	3	5	5
	(25°C)						
	90			2	5	-	5
	120	1	1	-	5	-	5
	200			2	3	-	-
	300			2	2	-	-
	400	2	2	2	2	-	-
	500			3	3	-	-
4	120				2		
	400	2	2				
6	120			2	2		
	400	2	2				
8	120			2	2		
	400	2	2				
10	120			2	2		
	400	2	2				
12	120			3	2		
	400	2	2				
13	120			1	2		
	400	2	1				
14	400	2	2				
15	400	2	2				

III. RESULTS

Influence of the specimen geometry

Using specimens with shorter gauge length helps to overcome the issue of an increasing temperature gradient ΔT with higher test temperatures that occurs in the Gleeble machine. Compared to a ΔT of 108°C at 400°C test temperature for the long specimen design, the reduced gauge length shows a ΔT of only 19°C at the same test temperature, see Figure 2.

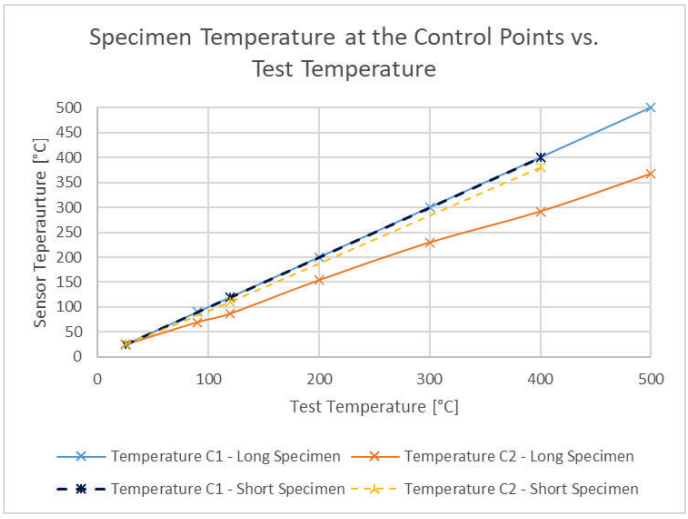

Fig. 2. Temperature measured at the thermocouple sensor placed in the middle (C1) and at the end (C2) of the gauge length for short and long specimen design

Figure 3 depicts strain curves at 120°C and 400°C for both specimen designs and heat treatments, and Figure 4 the ultimate tensile strength in comparison with MMPDS limits.

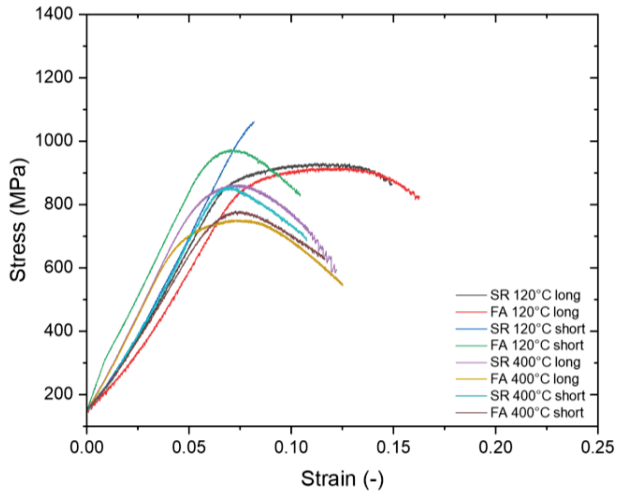

Fig. 3. Stress strain curves for long and short specimens at RT, 120°C and 400°C

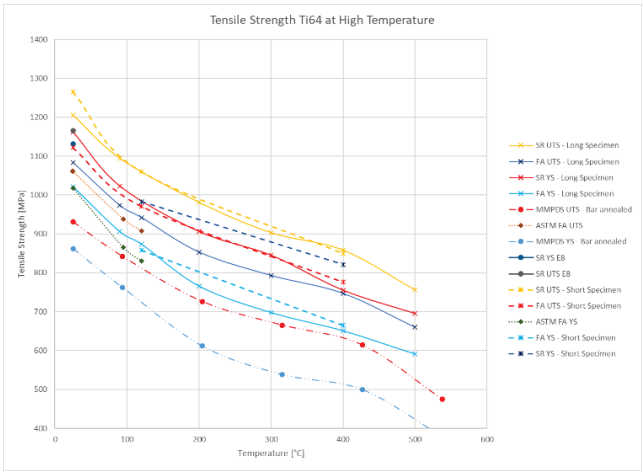

Fig. 4. Yield and ultimate tensile strength for different specimen design, heat treatment over the temperature, in comparison to MMPDS standards

At a test temperature of 400°C for which the short specimens design was intended ultimate tensile strength and yield strength are not significantly influenced by the specimen's gauge length. The elongation at break for short specimens however is reduced compared to the long design. From the measurement data a rough correlation of 5-10% higher max strain for the longer design can be assumed, but for an empiric proof and mathematical model more data is needed (Figure 5).

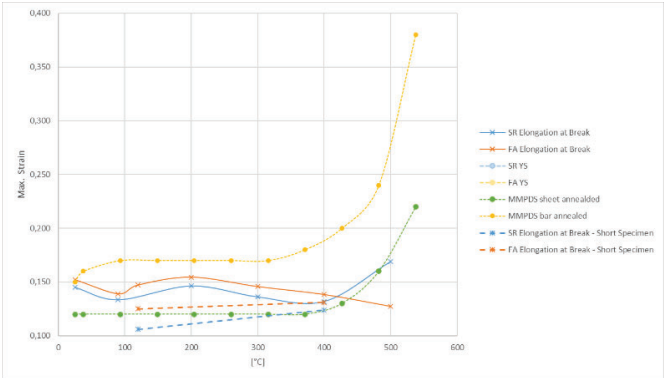

Fig. 5. Elongation at break for different specimen design, heat treatment over the temperature, in comparison to MMPDS standards specimen design

At 120°C yield strength is comparable while ultimate tensile strength is higher but the elongation significantly shortened. The reason for this may be due to the notches implemented for the additional gauge of the Gleeble system.

In both cases the non-linear behavior in the first fifth of the stress strain curves is caused by the conical clamping system used in the Gleebe machine, hence the values for the maximal strain have to be adapted accordingly.

Change in chemical composition

Table 2 shows the impact of the reuse cycles on the chemical composition of the powder. As described in the previous work [4], the increase of oxygen is caused by increasing oxide layers on the powder particles surface rather than dissolved oxygen inside the particles.

Tab. 2. Chemical composition of the powder over the reuse cycles [4]

Build Job	Al	H	N	O	Ar
	[wt. %]	[ppm]	[wt. %]	[wt. %]	[ppm]
Virgin	6.36	38	0.014	0.14	0.05
1	6.32	33	0.014	0.14	0.26
5	6.31	36	0.015	0.15	0.26
10	6.29	37	0.010	0.14	0.26
15	6.28	36	0.012	0.14	0.29
18	6.28	39	0.015	0.16	0.33
Limits Grade 5 (ASTM B265)	5.50-6.50	125	0.05	0.20	100

Microstructure

This growing oxide layer leads to a marginal drop in material density but no visible change in microstructure (Fig 6). With the available means of scanning electron microscopy, the traces of titanium oxide could not be detected.

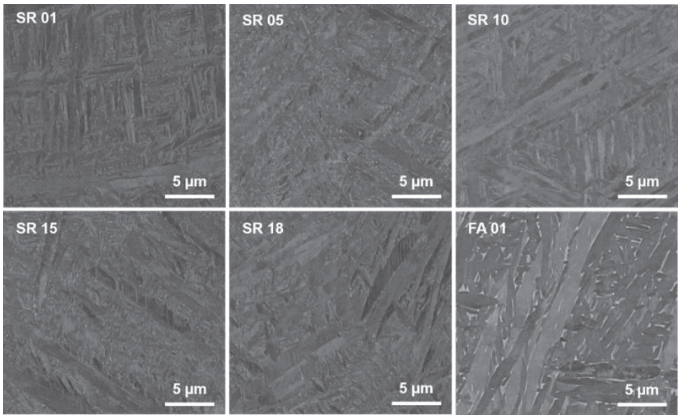

Fig. 6. Microstructure after 1, 5, 10, 15, and 18 reuse cycles for stress relieved specimen and for furnace annealed samples [4]

High temperature tensile properties

Figure 7 depicts the yield and ultimate tensile strength at RT, 120°C and 400°C over the reuse cycles, while Figure 8 shows stress strain curves optioned at 120°C (long specimen design) and Figure 9 at 400°C (short specimen design). In both figures results for stress relieved and furnace annealed

samples can be found.

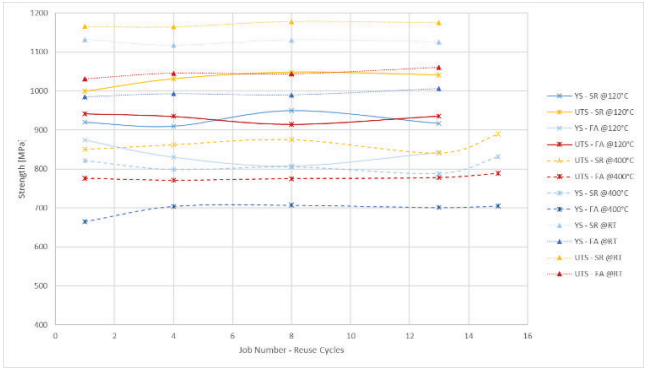

Fig. 7. Ultimate tensile and yield strength for, RT, 120° and 400°C over 13 (long specimen) and 15 reuse cycles (short specimen)

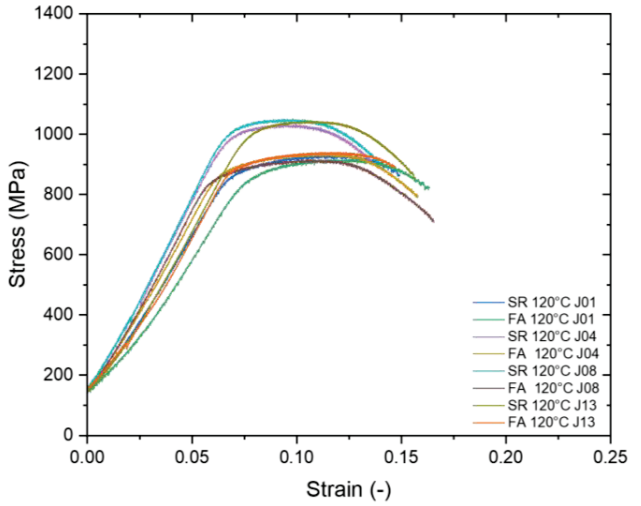

Fig. 8. Stress strain curves short specimens at 400°C in stress and furnace annealed condition for different reuse states.

At room temperature no measurable influence of the reuse on the tensile strength was observed [4]. Similar to this, at the temperatures of 120°C and 400°C the reuse cycles show no significant effect on the tensile properties. Therefore, the measured increase in titanium oxide on the powder particles does not have an impact on the tensile strength in the investigated temperature window. As shown in the work before the martensitic microstructure leads to higher strength at elevated temperature with comparable ductility at 120°C and 400°C.

Hence the reuse of powder shows no significant impact on the tensile properties of Ti64 within the useable temperature range suggested in standards and literature

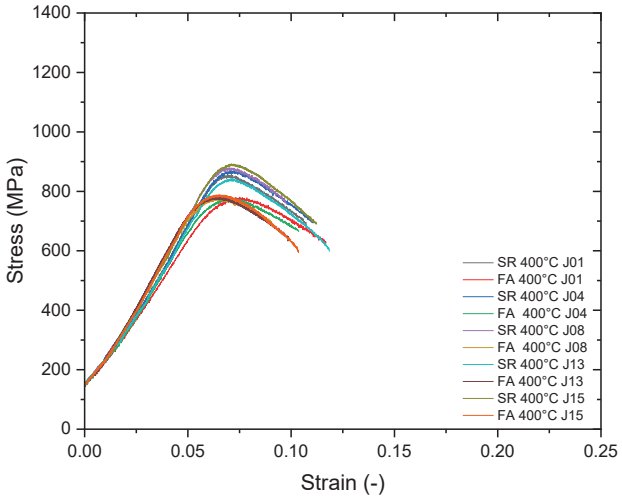

Fig. 9. Stress strain curves short specimens at 400°C in stress and furnace annealed condition for different reuse states.

IV. Conclusions and Future Work

The short specimen design introduced in this work allows to reduce the temperature gradient in samples from materials with low thermal conductivity in the Gleeble system. The design proves useful for higher temperatures with comparable results for yield strength and ultimate tensile strength and a correlating elongation at break, however, at lower temperatures only yield strength values could be directly compared. Ultimate tensile strength was higher while the maximal strain was significantly lower. This might be due to the notches in the design implemented to hold the Gleeble specific extensometer. Additional investigations are needed to clear these issues.

To receive results overall comparable to ISO/ASTM standards it is necessary to perform according standardized benchmark tests. A higher number of test data would help to establish an empirically approved formula especially needed for the correlation of the maximal strain between the different gauge lengths.

For the economically crucial topic of powder reuse in L-PBF the results show that the reuse of powder has no significant impact on the high temperature tensile properties of Ti64 within the allowed temperature range suggested in standards and literature. Of course, this can only be achieved with accurate process and material handling, quality powder feedstock and in standardized working conditions. Therefore, a regular monitoring of these influence factors and the achieved material properties is necessary.

Concerning the high temperature strength of Ti64 processed by L-PBF a number of questions remain open for future research:

Similar as found in the studies for α-Titanium alloys the heat treatment of Ti64 could be optimized for high temperature applications. Additionally, a deeper investigation of creep and fatigue properties at elevated temperatures might be necessary, also in connection with process parameters, as the trend towards larger layer thicknesses for productivity increases the as-build grain size.

For the possible application of L-PBF processed Ti64 at temperatures above 400°C the stability of the favorable martensitic microstructure at the desired working temperatures has to be studied.

ACKNOWLEDGEMENT

This work was partially supported by the Federal Ministry Republic of Austria, Climate Action, Environment, Energy, Mobility, Innovation, and Technology, Austrian Research Promotion Agency program Take-off, grant number 861050 and grant number 3859424 and measurements where conducted during the PhD Thesis of the main author at IMAT Institute of Material Science, Joining and Forming, Graz University of Technology, Graz, Austria with support of Joanneum Research – Materials, Niklasdorf, Austria.

REFERENCES

[1] Henri Paris, Hossein Mokhtarian, Eric Coatanea, Matthieu Museau, Inigo Flores Ituarte; comparative environmental impacts of additive and subtractive manufacturing technologies, CIRP Ann. Manuf. Technol. 65 (2016) 29–32.

[2] W.R. Morrow, H. Qi, I. Kim, J. Mazumder, S.J. Skerlos, Environmental aspects of laser-based and conventional tool and die manufacturing, J. Clean. Prod. 15 (2007) 932e943.

[3] Runze Huang, Matthew Riddle, Diane Graziano, Joshua Warren, Sujit Das, Sachin Nimbalkar, Joe Cresko, Eric Masanet, Energy and emissions saving potential of additive manufacturing: the case of lightweight aircraft components, J. Clean. Prod. 135 (2016) 1559e1570.

[4] Benjamin Meier, Fernando Warchomicka, Daniela Ehgartner, Denis Schuetz, Paul Angerer, Jaroslaw Wosik, Carlos Belei, Jelena Petrusa, Reinhard Kaindl, Wolfgang Waldhauser, Christof Sommitsch; Toward a sustainable laser powder bed fusion of Ti 6Al 4 V: Powder reuse and its effects on material properties during a single batch regime; Journal: Sustainable Materials and Technologies Volume 36, July 2023, e00626; https://doi.org/10.1016/j.susmat.2023.e00626

[6] Leyens, C.; Peters, M. Titanium and Titanium Alloys; Wiley-VCH Verlag: Hoboken, NJ, USA, 2003; ISBN 3-527-30534-3.

[7] G. Lütjering, J.C.Williams; Titanium; Springer; 2nd Edition

[8] Metallic Materials Properties Development and Standardization (MMPDS)-06, 2001, Chapter 5.4.1

[9] Benjamin Meier, Fernando Warchomicka, Jelena Petrusa, Reinhard Kaindl, Wolfgang Waldhauser, Christof Sommitsch; High Temperature Tensile Strength of Ti6Al4V Processed By L-PBF – Influence Of Microstructure And Heat Treatment; Proceedings of the Metal Additive Manufacturing Conference 2022 and BHM Berg- und Hüttenmännische Monatshefte 2023,

[10] Luigi Mario Viespoli, Stefano Bressan, Takamoto Itoh, Noritake Hiyoshi, Konda Gokuldoss Prashanth, Filippo Berto; Creep and high temperature fatigue performance of as build selective laser melted Ti-based 6Al-4V titanium alloy; Engineering Failure Analysis 111 (2020) 104477; https://doi.org/10.1016/j.engfailanal.2020.104477

[11] Leuders, S.; Thöne, M.; Riemer, A.; Niendorf, T.; Tröster, T.; Richard, H.A.; Maier, H.J. On the mechanical behaviour of titanium alloy TiAl6V4 manufactured by selective laser melting: Fatigue resistance and crack growth performance. Int. J. Fatigue 2013, 48, 300–307.

[12] Benjamin Meier, Fernando Warchomicka, Reinhard Kaindl, Christof Sommitsch & Wolfgang Waldhauser; Influence of Different Surface- and Heat Treatments; Elevated Temperature, Orientation on the Fatigue Properties of Ti6Al4V processed by L-PBF for Controlled Powder Properties; Lesiuk, G., Duda, S., Correia, J.A.F.O., De Jesus, A.M.P. (eds) Fatigue and Fracture of Materials and Structures. Structural Integrity, vol 24. Springer, Cham.; https://doi.org/10.1007/978-3-030-97822-8_27

[13] Meishen Xie, Sheng Huang, Zhi Wang, Upadrasta Ramamurty; High-temperature fracture behavior of an α/β Titanium alloy manufactured using laser powder bed fusion; Acta Materialia 277 (2024) 120211; https://doi.org/10.1016/j.actamat.2024.120211

[14] Jiachen Zhou , Baoxian Su, Guoqiang Zhu, Yinling Jin, Binbin Wang, Liangshun Luo, Ruirun Chen, Liang Wang, Qian Yang, Yongsheng Yu, Yanqing Su; High-temperature tensile properties of laser powder bed fusion Ti–6.5Al–2Zr–1Mo–1V alloy after annealing; Materials Science & Engineering A 923 (2025) 147700; https://doi.org/10.1016/j.msea.2024.147700

[15] Jianwen Liu, Yixin Li, Yuman Zhu, Yi Yang, Ruifeng Zhang, Zhenbo Zhang, Aijun Huang, Kai Zhang; Enhancing high-temperature strength and ductility in laser powder bed fusion Ti–6.5Al–2Zr–1Mo–1V alloy via heat treatment optimization; Materials Science & Engineering A 859 (2022) 144201: https://doi.org/10.1016/j.msea.2022.144201

[16] Riccardo Casati, Gabriele Boari, Alessandro Rizzi, Maurizio Vedani; Effect of annealing temperature on microstructure and high-temperature tensile behaviour of Ti-6242S alloy produced by Laser Powder Bed Fusion, European Journal of Materials, (2021) 1:1, 72-83, DOI: 10.1080/26889277.2021.1997341

[17] Zhiyang Kong, Tongsheng Deng, Hao Zhang, Yongjian Zheng, Ziziang Qiu, Haixuan wang, Yang Yang, Yaoyao Ding, Liwen Liang, Shimin Fang, Miaocheng Tian, Chaoyue Tang, Roman Mishnev; The optimization of high-temperature mechanical properties and microstructure evolution in laser powder bed fusion processed TC17 titanium alloy; preprint; https://ssrn.com/abstract=5231108

[18] Sagar Patel, Mohsen Keshavarz, Mihaela Vlasea; Challenges during laser powder bed fusion of a near-alpha titanium alloy - Ti-6242Si; Solid Freeform Fabrication 2021: Proceedings of the 32nd Annual International Solid Freeform Fabrication Symposium – An Additive Manufacturing Conference - Reviewed Paper

[19] Shuhan Li, Xinqiang Lan, Zemin Wang, Shuwen Mei; Microstructure and mechanical properties of Ti-6.5Al-2Zr-Mo-V alloy processed by Laser Powder Bed Fusion and subsequent heat treatments; Additive Manufacturing 48 (2021) 102382; https://doi.org/10.1016/j.addma.2021.102382

Mechanical Properties of Carbon and Natural Fibers - TPU Composites for Additive Manufacturing Applications

Jaka Vaupot[1], Tomaž Lampe[2], Janez Slapnik[3], Sandra Schulnig[4], Andrijana Sever Škapin[1,3]*

Slovenian National Building and Civil Engineering Institute,
Dimičeva ulica 12, 1000 Ljubljana, Slovenia[1]
Faculty of Health Sciences, University of Ljubljana, Zdravstvena Pot 5, 1000 Ljubljana, Slovenia[2]
Faculty of Polymer Technology – FTPO, Ozare 19, 2380 Slovenj Gradec, Slovenia[3]
ADMiRE Research Center, Carinthia University
of Applied Sciences, Villach, Austria[4]
Corresponding Author: andrijana.skapin@zag.si*

Abstract—**This research aims to address the performance gap between traditional synthetic fiber composites and their natural counterparts by tailoring the mechanical and functional properties of bio-composites, with a particular focus on bio-based polymer matrices TPU reinforced with natural and carbon fibers. The goal is to develop sustainable materials for functional applications in the medical field (e.g., prosthetics and orthotics), utilizing fused deposition modeling (FDM) as a flexible and personalized manufacturing method.**

I. Introduction

Fiber-reinforced polymer (FRP) composites have become an important part of modern materials science due to their good strength-to-weight ratio, corrosion resistance and design flexibility. Thermoplastic-based FRPs are particularly promising as they are recyclable, processable and compatible with advanced molding processes such as 3D printing. In recent years, the integration of natural fibers into polymer matrices (N-FRP) has gained momentum. This has been driven by environmental concerns, the growing interest in bio-based materials and the principles of the circular economy [1,2].

Natural fibers offer several advantages over conventional reinforcement materials such as glass or carbon fibers, including low density, renewability, biodegradability and cost efficiency [3]. However, their wider application is often limited by problems such as moisture absorption, variations in fiber quality and poor interfacial adhesion with hydrophobic thermoplastic matrices [4]. Research has shown that the incorporation of natural fibers into thermoplastic matrices can significantly improve tensile and flexural strength, modulus and hardness - but usually at the expense of lower impact strength and ductility [5,6]. There is usually an optimum content of fibers beyond which the mechanical properties tend to plateau or deteriorate due to poor dispersion or saturation of the matrix [7].

The mechanical performance of composite materials is influenced by several parameters, including the volume fraction of fibers, their length, orientation and the interfacial bonding between fiber and matrix. Studies confirm that even short carbon fibers (CF) and natural fibers, when used correctly, can improve the modulus and strength of bio-based thermoplastic matrices such as TPU or PLA [5,6,8]. For example, composites with 5–15 wt% carbon fibers show significant increases in stiffness and tensile strength, especially when longer fibers (~150 μm) are used [5]. For natural fibers such as kenaf or hemp, the optimum proportion is typically between 20–30 wt% and offers a good balance between mechanical performance and processability [6]. However, the degree of reinforcement strongly depends on the compatibility between fibers and matrix. A variety of surface modification techniques including alkaline treatment, silane coupling and plasma treatment have been investigated to improve interfacial bonding and reduce water absorption [4,7].

II. Additive Manufacturing of Biocomposites

Additive manufacturing (AM), particularly the Fused Filament Fabrication (FFF) process, offers a promising route to produce customized, lightweight and functional parts from bio-composites. While FFF offers great design freedom and material efficiency, it also brings new challenges, such as fiber breakage during extrusion, anisotropy, layer delamination and porosity. These factors are influenced by printing parameters such as nozzle temperature, filling density, printing speed and layer height [9].

Despite the increasing interest in bio-composites for AM, most studies focus on isolated aspects such as tensile or thermal behavior and often neglect the broader interactions between material formulation, printing process and the

functionality of the finished part. There is a lack of integrated methods linking materials design, extrusion processing and AM performance, especially for real-world applications [10].

III. Application Case: Fiber-Reinforced TPU for Orthotic Insole

This study focuses on the development of bio-based TPU composites reinforced with carbon and cellulose fibers and aims at applications in customized orthopedic insoles. TPU is widely used for orthopedic insoles due to its elasticity, softness and biocompatibility, but its low stiffness and limited wear resistance reduce its durability in long-term use. Fiber reinforcement offers a way to mechanically improve TPU while maintaining sufficient flexibility for comfort.

A total of six composite formulations of bio-based TPU with 10, 15 and 20 wt% carbon or cellulose fibers were produced using a co-rotating twin-screw extruder. To ensure consistency and minimize moisture-related defects, the composite pellets were dried at 80 °C for 12 hours prior to extrusion. Filaments with a diameter of 1.75 mm were produced using a special extrusion line and then printed using the FFF 3D printing process to prepare standardized test specimens for mechanical analysis, which were evaluated using tensile, compression tests and Shore A hardness measurements. Since insoles need to consist of regions with different mechanical requirements, e.g. hardness, we printed compression test specimens with different infill (15 %, 40 %, 60 %, and 95 %).

The tensile tests showed that both carbon and cellulose fibers enhanced the tensile modulus of elasticity compared to neat TPU. The composites of carbon and cellulose fibers showed the most significant improvement in stiffness, with the formulation containing 20 wt% fibers achieving the highest tensile modulus (Fig. 1). However, the sample with 20 wt% fibers showed the most signs of embrittlement, which was reflected in a lower elongation at break (Fig. 2). An increase in fiber content results in a continuous rise in tensile modulus, accompanied by a reduction in elongation at break.

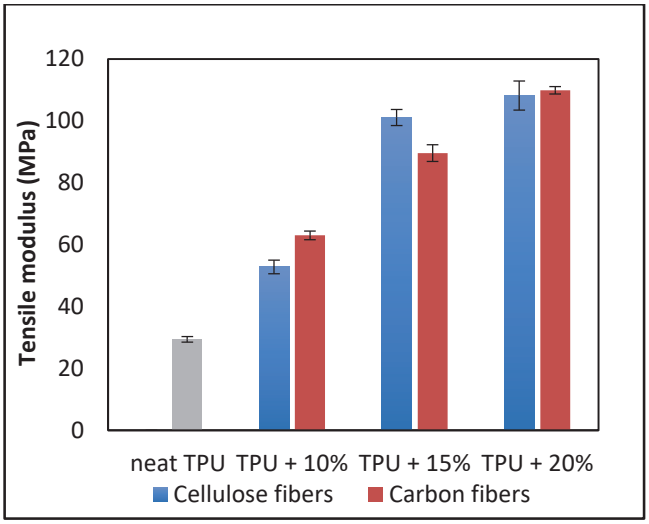

Fig. 1. The effect of fiber content in TPU composites on the tensile modulus.

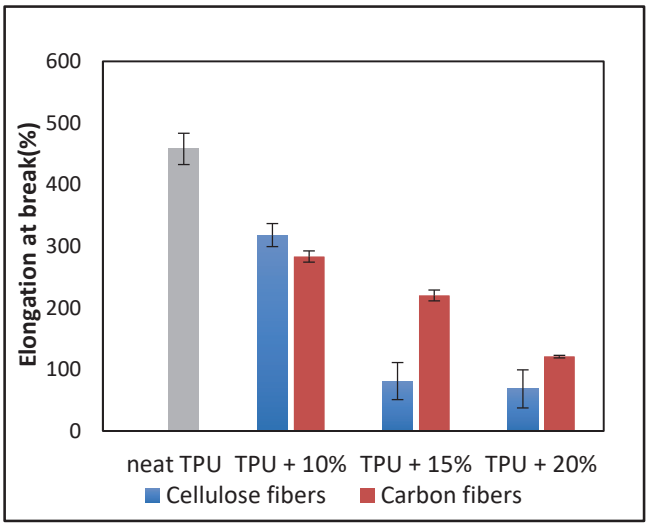

Fig. 2. The effect of fiber content in TPU composites on the elongation at break (tensile test).

Compression tests were performed on test specimens with 10, 15 and 20 % by weight carbon (a) and cellulose fibers (b) and with different infills (15, 40, 60 and 95 %). Fig. 2 shows that increasing the infill percentage leads to an exponential increase in the compression modulus for both fibers. The highest compression modulus was achieved at 15 wt% reinforcement for all composite samples produced (Fig. 3). It was also found that the best balance between stiffness and ductility was at 15 wt%.

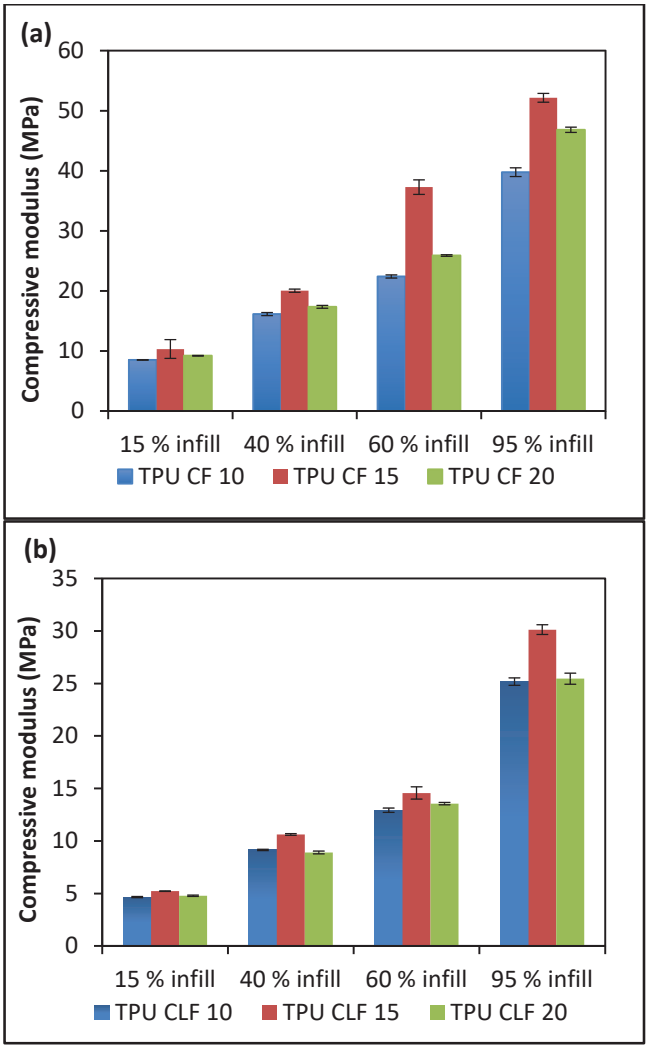

Fig. 3. Effect of fiber content in TPU–Carbon (a) and TPU–Cellulose (b) composites and infill percentage on compressive modulus

Shore A hardness increased with fiber content for both carbon and cellulose fibers composites (Fig 3). TPU + 20% carbon fibers by weight showed the highest Shore A value, indicating improved resistance to surface indentations - important for load-bearing orthopedic applications.

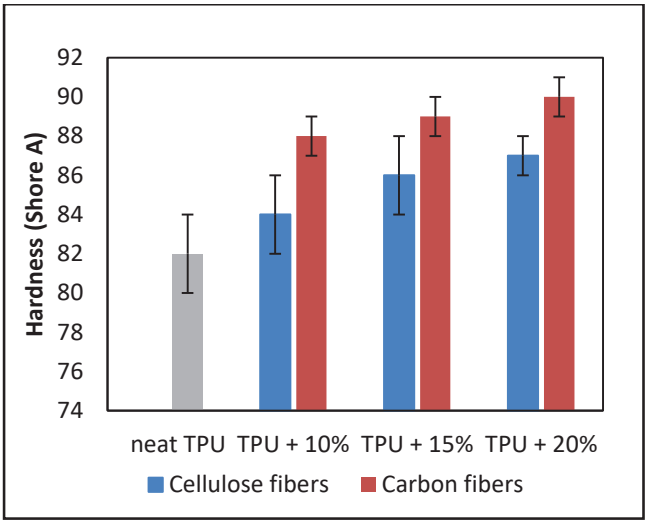

Fig. 4. The effect of fiber content in TPU composites on the Shore A hardness.

IV. Conclusions and Future Work

This study demonstrates the potential of bio-based TPU composites reinforced with carbon and cellulose fibers for additive manufacturing applications. Using a co-rotating twin-screw extruder, filaments containing 10–20% by weight of one of the two fiber types were successfully produced and processed into test specimens using FFF 3D printing. Mechanical tests showed that both fiber types significantly improved the tensile and compression properties, with the clearest improvements being observed at a proportion of 15% by weight. Shore A hardness also increased with fiber content.

The carbon fiber composites consistently outperformed their cellulosic counterparts in terms of modulus and strength, while cellulose-reinforced TPU exhibited better ductility. These results confirm that it is possible to control mechanical performance via fiber type and fiber content, making such composites suitable for customized, functional components- such as orthopedic insoles- produced by 3D printing.

Future work will focus on evaluating long-term performance under cyclical loading to simulate real-world use conditions, as well as further optimizing printing parameters and integrating fibers from waste materials to improve recyclability.

Acknowledgement

This work is part of the project “Promoting Sustainable Regional Development through Additive Manufacturing: A Cross-Border Initiative for a Resilient and Circular Economy” (ADDCIRCLES). The authors gratefully acknowledge the financial support for this research from the Interreg Programme Slovenia-Austria 2021-2027, co-funded by the European Union through the European Regional Development Fund (ERDF) under grant agreement no. SIAT00036 and by the internal interdisciplinary initiative DF Hub2 horizontal project. Authors also acknowledge the financial support by the Slovenian Research and Innovation Agency (Grants no. P2-0273) and by the internal

interdisciplinary initiative DF Hub2 horizontal project.

REFERENCES

[1] O. Faruk, A. K. Bledzki, H.-P. Fink, and M. Sain, "Biocomposites reinforced with natural fibers: 2000–2010," *Progress in Polymer Science*, vol. 37, no. 11, pp. 1552–1596, 2012.

[2] K. G. Satyanarayana, G. G. C. Arizaga, and F. Wypych, "Natural fiber–polymer composites," *Journal of Applied Polymer Science*, vol. 114, no. 1, pp. 1–15, 2009.

[3] P. Wambua, J. Ivens, and I. Verpoest, "Natural fibres: Can they replace glass in fibre reinforced plastics?" *Composites Science and Technology*, vol. 63, no. 9, pp. 1259–1264, 2003.

[4] A. K. Bledzki and J. Gassan, "Composites reinforced with cellulose-based fibres," *Progress in Polymer Science*, vol. 24, no. 2, pp. 221–274, 1999.

[5] H. Ning, W. Cong, J. Qiu, J. Wei, and M. Wang, "Effects of short carbon fiber reinforcement on the properties of 3D printed thermoplastic composites," *Composites Part B: Engineering*, vol. 80, pp. 369–378, 2015.

[6] Y. A. El-Shekeil, S. M. Sapuan, M. Jawaid, and Z. M. Leman, "Tensile and morphological properties of kenaf fiber reinforced thermoplastic polyurethane composites," *Materials & Design*, vol. 40, pp. 299–303, 2012.

[7] K. L. Pickering, M. G. A. Efendy, and T. M. Le, "A review of recent developments in natural fibre composites and their mechanical performance," *Composites Part A: Applied Science and Manufacturing*, vol. 83, pp. 98–112, 2016.

[8] S. Vivekanandhan, R. S. Misra, and M. Misra, "Mechanical performance of carbon fiber reinforced bio-based polytrimethylene terephthalate composites," *Composites Part B: Engineering*, vol. 45, no. 1, pp. 1113–1121, 2013.

[9] M. Domingo-Espin, J. A. Puigoriol-Forcada, A. Garcia-Granada, J. Llumà, J. A. Antoni Gil, and E. Borràs, "Influence of process parameters on mechanical properties of FDM parts," *Rapid Prototyping Journal*, vol. 21, no. 4, pp. 524–532, 2015.

[10] A. Arora and V. Sharma, "AI in Materials Design," *Advanced Materials*, vol. 32, no. 13, p. 1905539, 2020.

Tuning Quasi-Zero Stiffness in Additively Manufactured Kresling Structures via Silicone Encapsulation and Infill Design

Carina Emminger[1]*, Martin Reiter[1], Umut Cakmak[1], Zoltan Major[1]

Johannes Kepler Universtiy Linz, Institute of Polymer Product Engineering, Linz, Austria[1]
Corresponding Author: carina.emminger@jku.at*

Abstract—**Origami-inspired metamaterials enable lightweight, reconfigurable structures with tunable properties. The Kresling pattern is of particular interest for its bistability and potential to realize quasi-zero stiffness (QZS) behavior. In this work, Kresling specimens were fabricated from thermoplastic poly(urethane) (TPU) using fused filament fabrication (FFF) and modified by silicone overcasting with poly(dimethylsiloxane) (PDMS) layers of varying thickness and hardness. Uniaxial compression tests showed that PDMS encapsulation increases overall stiffness and load-bearing capacity but reduces the extent of the QZS region. Infill density variations provided an additional means of tuning: lower densities promoted broader QZS regimes, while higher densities enhanced stiffness at the expense of tunability. The results demonstrate that combining additive manufacturing with silicone encapsulation and infill design offers complementary strategies to program the mechanical response of Kresling structures. This hybrid approach enables the development of origami-based metamaterials tailored for vibration isolation, damping, and soft robotic applications.**

I. Introduction

Origami-inspired metamaterials use folding principles to achieve lightweight, reconfigurable, and tunable structures [1], [8], [9]. The Kresling pattern is a well-studied example, notable for its bistability and collapsibility [2], [3], [6]. These features make it relevant for deployable systems, damping, and soft robotics [7], [9].

Additive manufacturing (AM), especially fused filament fabrication (FFF), extends origami research beyond paper or thin films [4], [5]. Flexible thermoplastic poly(urethane) (TPU) allows Kresling structures that combine elasticity with geometric stability. However, most 3D printed prototypes remain monolithic, limiting their mechanical tunability.

Quasi-zero stiffness (QZS) is particularly attractive for vibration isolation, damping, and adaptive devices [3], [4]. In this regime, a structure maintains stability while offering minimal resistance over part of its deformation range. Kresling geometries can realize QZS, but the effect is highly sensitive to geometry, material, and fabrication method.

Prior work has largely addressed idealized models or single-material Kresling structures [2], [6]. While QZS behavior is recognized, its precise modulation is difficult. The influence of infill design in printed walls is also underexplored, and the role of soft encapsulation with silicone remains largely unstudied.

This study fabricates Kresling structures in TPU using FFF and applies silicone overcasting to tune QZS regions. Different wall infill patterns and density are also tested to evaluate their effect on stiffness and deformation. The approach integrates AM with soft encapsulation and geometric tuning.

II. EXPERIMENTAL

Parametric CAD models of Kresling structures were created to vary polygon type, side angle, wall thickness, and height. For this study, hexagonal and octagonal patterns with a diameter of 35 mm, wall thickness of 1 mm, and height of 20 mm were selected as reference geometries.

The specimens were produced by FFF using a Rat Rig Core v4 500 printer equipped with a 0.6 mm nozzle. TPU (Extrudr Medium) was processed at 240 °C with a 50 °C heated bed. To investigate the influence of wall architecture, infill density was varied between 5% and 50% in 5% steps.

Encapsulation was performed by overcasting the printed structures with poly(dimethylsiloxane) (PDMS). Two formulations were employed: Dragon Skin 30 (Shore A30, Smooth-On Inc.) and Ecoflex 00-30 (Shore 00-30, Smooth-On Inc.). The PDMS layer thickness was varied from 1 mm to 4 mm in steps of 1 mm.

Mechanical characterization was carried out under displacement-controlled uniaxial compression using a Zwick Roell LTM 10t multiaxial testing system. Force–displacement data were recorded to evaluate stiffness, deformation behavior, and the extent of the QZS region.

III. RESULTS

Compression tests highlight the influence of silicone encapsulation on the mechanical response of the TPU

Kresling structures. Figure 1 compares the force–displacement behavior of a hexagonal Kresling with and without a 4 mm Ecoflex 00-30 layer. Both specimens exhibit similar stiffness prior to the onset of the quasi-zero stiffness (QZS) region. However, the encapsulated structure shows a notably higher force level throughout loading and a QZS range reduced by nearly 50%.

The increase in overall compression force is attributed to the effective thickening of the walls by the PDMS layer, which restricts deformation. While this reduces the displacement interval over which QZS is observed, it enables higher load-bearing capacity. These results confirm that combining TPU with softer PDMS allows for tailoring the balance between compliance and stiffness.

Preliminary tests on different infill densities further suggest that wall architecture significantly affects force levels and the stability of the QZS regime. Lower infill densities promote broader QZS ranges, while higher densities increase overall stiffness at the cost of reduced tunability. Together, the findings demonstrate that both silicone encapsulation and infill design provide complementary levers to program the mechanical response of Kresling structures.

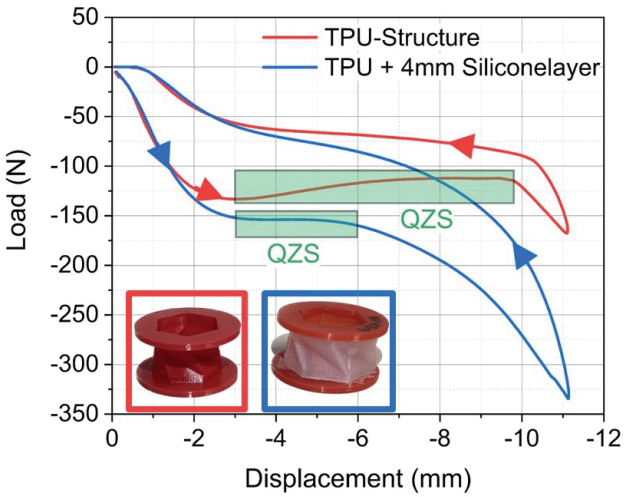

Fig. 1. Force – compressive displacement curves of the TPU Kresling pattern in comparison to the influence of a 4mm thick PDMS (Ecoflex 00-30) encapsulation. The PDMS-Layer causes a decrease of the QZS range and an increase in the overall compression force compared to the TPU structure without PDMS.

IV. Conclusions and Future Work

This study demonstrates that additively manufactured Kresling structures in TPU can be effectively modified through silicone encapsulation and infill design to alter their mechanical response. Compression tests revealed that PDMS layers increase overall stiffness and reduce the range of quasi-zero stiffness, while maintaining the potential for tunable behavior. The combination of flexible 3D printing and soft overcasting thus provides a viable pathway to engineer structures with tailored deformation and stiffness characteristics.

Future work will focus on systematically mapping the influence of PDMS thickness, material properties, and infill geometries on the quasi-zero stiffness regime. Additional efforts will be directed toward cyclic loading tests to assess durability, and toward integrating these hybrid structures into application scenarios such as vibration isolation, damping, and adaptive soft robotic components.

Acknowledgement

The authors wish to acknowledge Lisa Klingersberger for her essential contribution to the conceptual development of this work. She introduced the Kresling pattern to the team and thereby providing the foundational idea for this study.

References

[1] Kresling, Biruta, and John F. Abel. "Natural twist buckling in shells: from the hawkmoth's bellows to the deployable Kresling-pattern and cylindrical Miura-ori."*Proceedings of the 6th international conference on computation of shell and spatial structures*. Vol. 11. International Association for Shell and Spatial Structures, Ithaca, NY, 2008.

[2] Kidambi, N., and K. W. Wang. "Dynamics of Kresling origami deployment."*Physical Review E* 101.6 (2020): 063003.

[3] Joseph, Kevin Kuriakose, Ahmed S. Dalaq, and Mohammed F. Daqaq. "A Static Analysis of Compression and Torsion of Kresling Origami Springs." *10th World Congress on Mechanical, Chemical, and Material Engineering, MCM 2024*. Avestia Publishing, 2024.

[4] S. Mora, N. M. Pugno, and D. Misseroni, "Programming the energy landscape of 3D-printed Kresling origami via crease geometry and viscosity," *Extrem. Mech. Lett.*, vol. 77, p. 102314, Jun. 2025.

[5] D. C. Bershadsky and G. H. Paulino, "Framework for the fabrication of scalable, flat foldable, thick origami Kresling structures via non-rigid methods."

[6] J. Li, Y. Chen, X. Feng, J. Feng, and P. Sareh, "Computational modeling and energy absorption behavior of thin-walled tubes with the kresling origami pattern," *J. Int. Assoc. Shell Spat. Struct.*, vol. 62, no. 2, pp. 71–81, 2021.

[7] S. Ye, P. Zhao, Y. Zhao, F. Kavousi, H. Feng, and G. Hao, "A Novel Radially Closable Tubular Origami Structure (RC-ori) for Valves," *Actuators*, vol. 11, no. 9, Sep. 2022.

[8] G. W. Hunt and I. Ario, "Twist buckling and the foldable cylinder: an exercise in origami," *Int. J. Non. Linear. Mech.*, vol. 40, no. 6, pp. 833–843, Jul. 2005.

[9] J. Francis and V. Vincent, "Morpho-functional Machines: The New Species," *Morpho-functional Mach. New Species*, no. May, 2003.

TAILOR-MADE CONDUCTIVE THERMOPLASTIC FILAMENTS FOR EXTRUSION-BASED FLM PRINTED STRAIN SENSING IN THERMOSET COMPOSITES

Claudia Pretschuh*, Debasish Tamuli, Konrad Wipplinger, Arunjunai Raj Mahendran

All: Kompetenzzentrum Holz GmbH (WOOD K plus)
Altenberger Str. 69, 4040 Linz, Austria[1]
Corresponding Author: c.pretschuh@wood-kplus.at*

***Abstract*—Quality monitoring of composite products and especially of wooden composites requires the development of low-cost and stable sensors, which can be applied directly on surfaces or on thin carrier substrates. We present an innovative and new strain sensor fabrication method, applicable on wood and paper substrates, including the development of suitable electrically conductive thermoplastic filaments for extrusion-based Fused Layer Modeling (FLM) printing on very thin and flexible paper substrates.**

I. INTRODUCTION

For a successful embedding of sensors into thermoset composites, it is advantageous to develop thin and flexible sensors. Therefore, thin cellulosic papers are very suitable substrates. Considering the need for sustainable production, additive manufacturing techniques are also emerging to allow freedom in the design of sensor structures. While relatively new in the field of electronics, 3D printing is becoming more available for specialized applications. One benefit of digitally printed electronics is that they are easier processable than photochemically prepared components. The selection of an additive manufacturing technology instead of analogous screen-printing can avoid the demand for printing inks and the high demand for fossil-based solvents and cleaning agents.

In the presented approach, extrusion based FLM printing is applied for the development of thin strain sensors on cellulosic paper. Currently, only a few extruded filament types for printing of electrically sufficient conductive materials are available on the market [1]. The requirements for such filaments include sufficient processability, high and reliable electrical conductivity, and sufficient chemical and thermal stability of the printed conductive structures.

Limited choices in FLM feedstock materials hinders the applicability to new industrial fields; various types of relatively expensive functional fillers (carbon nanotubes CNTs, graphene) were used [2]. Readily accessible filaments with electrical conductivity exist, but they are still scarce, so FLM applications in the electronic field are limited. As one example with superior electrical performance, filaments based on PLA, traditional CNTs and lignin blends have been studied by combining solution mixing and melt blending [3]. However, the introduction of a plasticizing additive, lignin, was required. PLA has drawbacks for this application, such as lower ductility and its electrical insulating properties.

The potential variability of functional fillers and thermoplastic matrices adds complexity to the printing process as it differs from one filament to another; but these different properties can open the door to high potential applications. Commercially available conductive FDM filaments are currently based on PLA or TPU combined with either traditional carbon-black, graphene or CNTs [4]. These mentioned filaments can be used for EMG (electromyography) sensing, printing of electrodes, for strain or force sensors (resistive, capacitive or piezoresistive types) and even for the printing of antennas. Strain gauges can be further integrated into 3D printed prosthetic devices or into soft actuators in robotics, for haptic and touch feedback [5]; or they can be used for structural monitoring of different composite materials.

The specialized development of conductive filaments for sensor-based applications on thermoset composites include the following steps: twin screw compounding of a thermoplastic polymer with commercial conductive carbon fillers, filament extrusion, 3D printing of a resistive sensor on cellulosic paper, fixation on a composite and sensor validation during several loading cycles.

The aim of this study was to show the potential of solvent-free additive printing as manufacturing method for strain sensors required for structural health monitoring in the automotive sector. Therefore, different thermoplastic polyamide matrices (PA12, PA10.10, PA6) and conductive carbon black fillers have been selected (carbon black types, ENSACO and one Multiwall carbon nanotube MWCNT containing masterbatch Plasticyl PP2001).

II. EXPERIMENTAL WORK

Thermoplastic PA matrix has been compounded with different conductive fillers (diverse types of conductive carbon black, ENSACO) by using a parallel, co-rotating twin-screw compounder (20mm screw diameter). For

every PA type and filler type, the content of the filler was varied and optimized to obtain sufficient elastic and as well electrically conductive compounds. Throughput was between 1.2-3kg/h.

Compounds with a filler content between 20wt% and 40wt% were used for the subsequent filament extrusion. For this step, a conical, counter-rotating twin screw extruder was used in combination with a melt pump. Mass pressure was between 15-50bar. The filament passes through a water bath to cool down the filament temperature and to maintain its diameter at 1.75 mm, which is controlled after the cooling step. In the subsequent step, the filament is wound onto a spool with a constant pulling speed of 11m/min (Fig. 1).

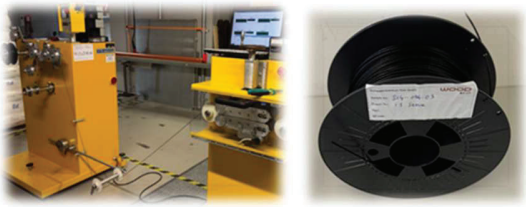

Fig. 1. Winding of extruded filament for FLM printing.

During the FLM printing at a Prusa i3 MK3S onto very thin cellulosic paper, the following printing parameters were used: an extruder temperature of 275°C, bed temperature of 30°C, printing speed of 5mm/s and a layer height of 0.3 mm. For the printing of conductive sensors, a continuous meander type structure was chosen (Fig. 2).

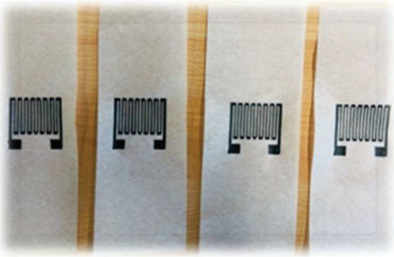

Fig. 2. Meander structure of resistive strain sensor, FLM printed on thin cellulosic papers.

For their evaluation, first cyclic tensile tests were performed on the 3D printed sensors. 6 most promising formulations were selected for these tests. Second, for flexural and cyclic bending tests, the printed paper sensors were laminated onto a fiber board using epoxy resin (Fig. 3).

III. RESULTS

Melt strands with brittle properties were excluded from filament extrusion, as they lack the necessary flexibility and elasticity. For the selected PA6 matrix, an increase of the filler content was required to enhance conductivity, and it compromised the elasticity needed for successful filament production. With the selected PA10.10 polymer, conductive compounds and filaments could be successfully prepared with a filler content of 20% and 30%. With the selected PA12 polymer, conductive and elastic compounds were prepared with a filler content of 30%.

In contrast to commercial thermoplastic polyurethane TPU or polylactic acid (PLA) based filaments, the developed PA12-based 3D printed sensors responded successfully after the lamination process. This improved chemical and thermal stability is derived from the change to a polyamide matrix material. During flexural load, the baseline decreased during the first 5 cycles and stayed constant afterwards (Fig. 4).

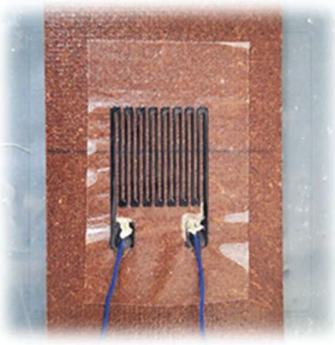

Fig. 3. 3D printed paper-based sensor, laminated with epoxy resins on a fiberboard.

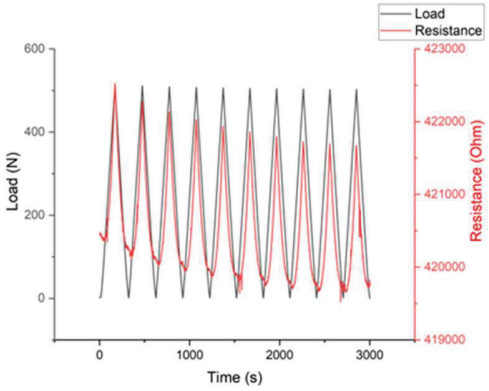

Fig. 4. Strain sensor evaluated via 3-point flexural testing. (filament: PA12-30% ENSACO 250G filled).

IV. CONCLUSION

Such easily printable and sufficient electrically conductive filaments can be used as a low-cost solution for the preparation of 3D FLM printed stable sensors. Potentially, the printing of different sensor types can be carried out in the future by using fully biobased and biodegradable thermoplastic materials. Conductive carbon-based fillers could be available as well from different plant based or recycled precursor materials.

3D FLM printing can be a successful possibility to establish new production processes in the field of sensorics and electronics. R&D steps in higher TRL levels will be required to develop promising and subsequently market-ready prototypes.

ACKNOWLEDGEMENT

The study was part of the COMET Module i³ Sense project: the Exploration of intelligent, integrated and impregnated cellulose-based sensors for load-bearing materials in construction, automotive, and sports industries. I³ Sense is a COMET Module within the COMET – Competence Centers for Excellent Technologies Program and funded by BMK, BMAW. COMET is managed by FFG. For the 3D FLM printing many thanks go to Master student Debasish Tamuli who performed a part of this work during his thesis; and as well to our colleagues Melanie Steiner for 3D printings and sensor validation; as well as to Mrs. Beste Kocoglu for data preparation and to Konrad Wipplinger for performing the compounding and extrusion process.

REFERENCES

[1] H. Watschke, K. Hilbig and T. Vietor, "Design and Characterization of Electrically Conductive Structures Additively Manufactured by Material Extrusion." Article in Applied Sciences, Vol. 9, 2019. Available: https://www.mdpi.com/2076-3417/9/4/779

[2] PM Angelopoulos, M Samouhos, M Taxiarchou. Functional fillers in composite filaments for fused filament fabrication; a review. Materials Today: Proceedings, Vol. 37, Part 4, 2021,4031-4043, ISSN 2214-7853, https://doi.org/10.1016/j.matpr.2020.07.069.

[3] Lage-Rivera, S.; Ares-Pernas, A.; Becerra Permuy, J.C.; Gosset, A.; Abad, M.-J. Enhancement of 3D Printability by FDM and Electrical Conductivity of PLA/MWCNT Filaments Using Lignin as Bio-Dispersant. Polymers 2023, 15, 999. https://doi.org/10.3390/polym15040999

[4] Aloqalaa, Z. Electrically Conductive Fused Deposition Modeling Filaments: Current Status and Medical Applications. Crystals 2022, 12, 1055. https://doi.org/10.3390/cryst12081055

[5] Elgeneidy K, Neumann G, Jackson M and Lohse N (2018) Directly Printable Flexible Strain Sensors for Bending and Contact Feedback of Soft Actuators. Front. Robot. AI 5:2. doi: 10.3389/frobt.2018.00002

The effect of the number of thermal cycles on the mechanical properties of parts fabricated by laser powder bed fusion

Snehashis Pal[1,2*], Tonica Bončina[1], Gorazd Lojen[1], Erika Švara Fabjan[3], Tomaž Brajlih[1], Nenad Gubeljak[1], Matjaž Finšgar[2], Igor Drstvenšek[1]

Faculty of Mechanical Engineering, University of Maribor, Maribor, Slovenia[1]
Faculty of Chemistry and Chemical Engineering, University of Maribor, Maribor, Slovenia[2]
Slovenian National Building and Civil Engineering Institute, Ljubljana, Slovenia[3]
Corresponding Author: snehashis.pal@um.si*

***Extended Abstract*—**The effect of thermal cycling on the thermal stress and crystallisation mechanism is the most important factor in determining the mechanical properties of parts manufactured by laser powder bed fusion. In this study, these mechanisms were investigated by changing the number of effective thermal cycles for different materials such as Ti-6Al-4V and Co-Cr-Mo alloys. The results showed remarkable differences in mechanical properties and microstructure. The microstructural differences were related to grain size, grain shape, grain boundary strength, crystal orientation, and crystal ordering. In particular, in Ti-6Al-4V, changes in martensitic size hierarchy, and in Co-Cr-Mo, proportional changes in coincidence site lattice (CSL) boundaries, were crucial in determining mechanical properties. Additionally, these crystal and grain formations differ not only in overall mechanical properties but also in different directions. They also determine the corrosion properties of the parts, which are crucial for biomedical applications [1].

A layer undergoes rapid heating and cooling several times during scanning itself and during the scanning of some subsequent layers [2]. Although the thermal effect of subsequent layers may be lower than the melting temperature, up to a few thermal cycles consisting of heating and cooling affect the material activity [3]. The number of effective thermal cycles was altered by changing the energy density and scanning speed. The laser power was varied between 55 W and 95 W, while the scanning speed was kept between 150 mm/s and 1000 mm/s for both alloys. The track overlap was 30% and the layer thickness was 25 μm. Their effects were analysed using microstructures, tensile tests, and microhardness measurements. In addition, differential thermal analysis (DTA) and heat treatment were used to reveal the mechanism of α'-martensite formation at different thermal cycles.

The proportion and orientation of α'-martensite differed significantly due to the changes in the number of thermal cycles. In addition, smaller to larger grains and irregular to classically hexagonal shaped grains appeared with increasing number of thermal cycles. The hierarchy with the size of α'-martensite also changed with the changes in thermal cycles. The proportion of quaternary α'-martensite varied the most with respect to other larger α'-martensites (tertiary to primary α'-martensites) [4]. A higher proportion of quaternary α'-martensite increased the hardness and modulus of elasticity. A lower proportion of primary and secondary α'-martensites meant that crack growth was not inhibited, resulting in a lower tensile strength. On the other hand, the grain size increased due to the increasing number of thermal cycles, which led to a deterioration in tensile strength. As a result, the yield strength deteriorated from 1200 MPa to 600 MPa, elongation fell from 8% to 2%, and the hardness ranged from 350 HV to 400 HV.

The combination of directional solidification and recrystallisation has remarkable effects on the grain boundary formation of the Co-Cr-Mo alloy [5], [6]. Directional solidification promoted the formation of CSL boundaries [7], while a higher number of effective thermal cycles caused an increase in CSL boundaries. In addition, a higher number of thermal cycles supported the transformation of γ-FCC (face-centred cubic) into HCP (hexagonal close-packed) martensite [8]. Since γ- FCC has sluggish nature of martensitic transformation in Co-Cr-Mo alloy [9], multiple thermal cycles enhance the time of martensitic transformation. On the other hand, the repeated rapid heating and cooling during production induces a thermal stress that intensifies the stress-induced martensitic transformation [10]. A higher proportion of martensite formation increased the yield strength and a higher proportion of CSL led to a longer plastic deformation under mechanical stress. Therefore, they improved the mechanical properties by increasing the yield strength from 700 MPa to 860 MPa and the elongation from 8% to 23%, which is particularly desirable for dental prosthesis applications.

Acknowledgement

The authors are grateful to the Slovenian Research and Innovation Agency for supporting this research. The grant numbers are P2-0118, P2-0137, P2-0157, P2-0120, P2-0273, J1-2470, J1-2471, J1-4416, J7-4636, J7-50226, J7-50227, J1-60015, J7-60120, and I0-0029.

References

[1] S. Pal, M. Finšgar, T. Bončina, G. Lojen, T. Brajlih, and I. Drstvenšek, "Effect of surface powder particles and morphologies on corrosion of Ti-6Al-4 V fabricated with different energy densities in selective laser melting," *Mater. Des.*, vol. 211, p. 110184, 2021, doi: https://doi.org/10.1016/j.matdes.2021.110184.

[2] J. Yang, H. Yu, J. Yin, M. Gao, Z. Wang, and X. Zeng, "Formation and control of martensite in Ti-6Al-4V alloy produced by selective laser melting," *Mater. Des.*, vol. 108, pp. 308–318, Oct. 2016, doi: http://dx.doi.org/10.1016/j.matdes.2016.06.117.

[3] S. Pal *et al.*, "Fine martensite and beta-grain variational effects on mechanical properties of Ti–6Al–4V while laser parameters change in laser powder bed fusion," *Mater. Sci. Eng. A*, vol. 892, p. 146052, 2024, doi: 10.1016/j.msea.2023.146052.

[4] S. Pal, G. Lojen, V. Kokol, and I. Drstvensek, "Evolution of metallurgical properties of Ti-6Al-4V alloy fabricated in different energy densities in the Selective Laser Melting technique," *J. Manuf. Process.*, vol. 35, pp. 538–546, Oct. 2018, doi: 10.1016/j.jmapro.2018.09.012.

[5] L. C. Chuang, K. Maeda, K. Shiga, H. Morito, and K. Fujiwara, "A {112}Σ3 grain boundary generated from the decomposition of a Σ9 grain boundary in multicrystalline silicon during directional solidification," *Scr. Mater.*, vol. 167, pp. 46–50, 2019, doi: 10.1016/j.scriptamat.2019.03.037.

[6] F. Lin, Y. Zhang, A. Godfrey, and D. Juul Jensen, "Twinning during recrystallization and its correlation with the deformation microstructure," *Scr. Mater.*, vol. 219, p. 114852, 2022, doi: 10.1016/j.scriptamat.2022.114852.

[7] T. Watanabe, "Approach To Grain Boundary Design for Strong and Ductile Polycrystals.," *Res Mech. Int. J. Struct. Mech. Mater. Sci.*, vol. 11, no. 1, pp. 47–84, 1984, [Online]. Available: https://www.scopus.com/inward/record.uri?eid=2-s2.0-0021214565&partnerID=40&md5=a5aa791020bf2a001b7307973918785a

[8] Z. Wang *et al.*, "Additive manufacturing of a martensitic Co–Cr–Mo alloy: Towards circumventing the strength–ductility trade-off," *Addit. Manuf.*, vol. 37, p. 101725, 2021, doi: 10.1016/j.addma.2020.101725.

[9] R. Turrubiates-Estrada, A. Salinas-Rodriguez, and H. F. Lopez, "FCC to HCP transformation kinetics in a Co-27Cr-5Mo-0.23C alloy," *J. Mater. Sci.*, vol. 46, no. 1, pp. 254–262, 2011, doi: 10.1007/s10853-010-4969-3.

[10] B. S. Lee, H. Matsumoto, and A. Chiba, "Fractures in tensile deformation of biomedical Co-Cr-Mo-N alloys," *Mater. Lett.*, vol. 65, no. 5, pp. 843–846, 2011, doi: 10.1016/j.matlet.2010.12.007.